

Spectroscopic Survey of X-type Asteroids¹

S. Fornasier^{1,2}, B. E. Clark³, E. Dotto⁴

¹ LESIA, Observatoire de Paris, 5 Place Jules Janssen, F-92195 Meudon Principal Cedex, France

² Univ. Paris Diderot, Sorbonne Paris Cité, 4 rue Elsa Morante, 75205 Paris Cedex 13

³ Department of Physics, Ithaca College, Ithaca, NY 14850, USA

⁴ INAF, Osservatorio Astronomico di Roma, via Frascati 33, I-00040 Monteporzio Catone (Roma), Italy

Submitted to Icarus: December 2010

e-mail: sonia.fornasier@obspm.fr; fax: +33145077144; phone: +33145077746

Manuscript pages: 38; Figures: 9; Tables: 7

Running head: Investigation of X-type asteroids

¹Based on observations carried out at the European Southern Observatory (ESO), La Silla, Chile, ESO proposals 074.C-0049 and 078.C-0115, at the Telescopio Nazionale Galileo, La Palma, Spain, and at the Mauna Kea NASA IRTF telescope, Hawaii, USA.

Send correspondence to:

Sonia Fornasier

LESIA-Observatoire de Paris

Batiment 17

5, Place Jules Janssen

92195 Meudon Cedex

France

e-mail: sonia.fornasier@obspm.fr

fax: +33145077144

phone: +33145077746

Spectroscopic Survey of X-type Asteroids¹

S. Fornasier^{1,2}, B. E. Clark³, E. Dotto⁴

Abstract

We present reflected light spectral observations from 0.4 to 2.5 μm of 24 asteroids chosen from the population of asteroids initially classified as Tholen X-type objects (Tholen, 1984). The X complex in the Tholen taxonomy comprises the E, M and P classes which have very different inferred mineralogies but which are spectrally similar to each other, with featureless spectra in visible wavelengths.

The data were obtained during several observing runs in the 2004-2007 years at the NTT, TNG and IRTF telescopes. Sixteen asteroids were observed in the visible and near-infrared wavelength range, seven objects in the visible wavelength range only, and one object in the near-infrared wavelength range only. We find a large variety of near-infrared spectral behaviors within the X class, and we identify weak absorption bands in spectra of 11 asteroids. Our spectra, together with albedos published by Tedesco et al. (2002), can be used to suggest new Tholen classifications for these objects. We describe 1 A-type (1122), 1 D-type (1328), 1 E-type (possibly, 3447 Burckhalter), 10 M-types (77, 92, 184, 337, 417, 741, 758, 1124, 1146 and 1355), 5 P-types (275, 463, 522, 909, 1902), and 6 C-types (50, 220, 223, 283, 517, and 536). In order to constrain the possible composition of these asteroids, we perform a least-squares search through the RELAB spectral

¹Based on observations carried out at the European Southern Observatory (ESO), La Silla, Chile, ESO proposals 074.C-0049 and 078.C-0115, at the Telescopio Nazionale Galileo, La Palma, Spain, and at the Mauna Kea NASA IRTF telescope, Hawaii, USA.

database. Many of the best fits are consistent with meteorite analogue materials suggested in the published literature. In fact, we find that 7 of the new M-types can be fit with metallic iron (or pallasite) materials, and that the low albedo C/P-type asteroids are best fitted with CM meteorites, some of which have been subjected to heating episodes or laser irradiation. Our method of searching for meteorite analogues emphasizes the spectral characteristics of brightness and shape, and de-emphasizes minor absorption bands. Indeed, faint absorption features like the $0.9\ \mu\text{m}$ band seen on 4 newly classified M-type asteroids are not reproduced by the iron meteorites. In these cases, we have searched for geographical mixture models that can fit the asteroid spectrum, minor bands, and albedo. We find that a few percent (less than 3%) of orthopyroxene added to iron or pallasite meteorite, results in good spectral matches, reproducing the weak spectral feature around $0.9\ \mu\text{m}$ seen on 92 Undina, 417 Suevia, and 1124 Stroobantia. For 337 Devosa, a mixture model that better reproduces its spectral behavior and the $0.9\ \mu\text{m}$ feature is made with Esquel pallasite enriched with goethite (2%).

Finally, we consider the sample of the X-type asteroids we have when we combine the present observations with previously published observations for a total of 72 bodies. This sample includes M and E-type asteroid data presented in Fornasier et al. (2008, 2010). We find that the mean visible spectral slopes for the different E, M and P Tholen classes are very similar, as expected. An analysis of the X-type asteroid distribution in the main belt is also reported, following both the Tholen and the Bus-DeMeo taxonomies (DeMeo et al. 2009).

Keywords: Asteroids, Surfaces, Spectroscopy, Meteorites

1. Introduction

The X complex in the Tholen taxonomy comprises the E, M and P classes which have very different inferred mineralogies but which are spectrally similar to each other and featureless in the visible wavelengths (Tholen, 1984). By convention X-types with measured geometric albedos are classified into Tholen E-type (high albedo, $p_v > 0.3$), M-type (medium albedo, $0.1 < p_v < 0.3$), or P-type (low albedo, $p_v < 0.1$) asteroids (Tholen&Barucci, 1989). The X-type asteroid indicates an "EMP" asteroid for which we do not have albedo information.

The X-type asteroids are distributed throughout the main belt (Mothé-Diniz et al. 2003) but tend to be concentrated around 3.0 AU, and in the Hungaria region (Warner et al. 2009). The X complex includes bodies with very different mineralogies. M asteroids may be composed of metals such as iron and nickel and may be the progenitors of differentiated iron-nickel meteorites (Gaffey, 1976; Cloutis et al. 1990, Gaffey et al. 1993). Enstatite chondrites have also been proposed as M-type asteroid analogs (Gaffey 1976; Vernazza et al. 2009; Fornasier et al. 2010; Ockert-Bell et al. 2010). A metallic iron interpretation requires that M asteroids are from differentiated parent bodies that were heated to at least 2000 °C to produce iron meteorites (Taylor, 1992).

E-type asteroids have high albedo values and their surface compositions are consistent with iron-free or iron-poor silicates such as enstatite, forsterite or feldspar. E-types are thought to be the parent bodies of the aubrite (enstatite achondrite) meteorites (Gaffey et al. 1989, Gaffey et al., 1992, Zellner et al., 1977, Clark et al. 2004a, Fornasier et al. 2008). P-type asteroids have low albedo values, and featureless red spectra. P-types are located mainly in the outer region of the main belt (Dahlgren & Lagerkvist 1995, Dahlgren et al. 1997, Gil-Hutton & Lican-

dro 2010) and in the Jupiter Trojan clouds (Fornasier et al. 2004, 2007a). They are probably primitive bodies, however they have no clear meteorite analogues. P-type asteroids are presumed to be similar to carbonaceous chondrites, but with a higher organic content to explain the strong red spectral slopes (Gaffey et al. 1989, Vilas et al. 1994).

In the last 15 years, several near-infrared spectral surveys have been devoted to the study of the X group and in particular the M and E-type asteroids, revealing that these bodies show great diversity in the infrared, even within the same class. In addition, polarimetric measurements (Lupishko & Belskaya 1989) and radar observations (Ostro et al., 1991, 2000; Margot and Brown, 2003; Magri et al., 2007; Shepard et al., 2008, 2010) of selected M-type asteroids have revealed surface properties that are in some cases inconsistent with metallic iron. Moreover, spectra of M-types are not uniformly featureless as initially believed; several spectral absorption bands have been detected in the visible and near infrared ranges. Faint absorption bands near 0.9 and 1.9 μm have been identified on the surfaces of some M-types (Hardersen et al., 2005; Clark et al., 2004b; Ockert-Bell et al., 2008; Fornasier et al., 2010), and of some E-type asteroids (Clark et al. 2004a; Fornasier et al. 2008) and attributed to orthopyroxene. A very peculiar absorption band, centered around 0.49-0.50 μm , extending from about 0.41 to 0.55 μm , was found on some E-type spectra (Burbine et al, 1998; Fornasier & Lazzarin, 2001; Clark et al. 2004a,b; Fornasier et al., 2007b, 2008), and attributed to the presence of sulfides such as troilite or oldhamite (Burbine et al., 1998, 2002a). Busarev (1998) detected weak features tentatively attributed to pyroxenes (at 0.51 μm) and oxidized or aqueously altered mafic silicates (at 0.62 and 0.7 μm) in the spectra of 2 M-type asteroids.

Of note is the evidence for hydrated minerals on the surfaces of some E and M-type asteroids (Jones et al, 1990; Rivkin et al, 1995, 2000, 2002), inferred from the identification of an absorption feature around $3\ \mu\text{m}$. This feature is typically attributed to the first overtone of H_2O and to OH vibrational fundamentals in hydrated silicates. If the origin of the $3\ \mu\text{m}$ band on E and M-type asteroids is actually due to hydrated minerals, then these objects are not all igneous as previously believed and the thermal scenario in the inner main belt would need revision. Gaffey et al. (2002) propose alternative explanations for the $3\ \mu\text{m}$ band: materials normally considered to be anhydrous containing structural OH; troilite, an anhydrous mineral that shows a feature at $3\ \mu\text{m}$, or xenolithic hydrous meteorite components on asteroid surfaces from impacts and solar wind implanted H. Rivkin et al. (2002) provide arguments refuting the Gaffey suggestions, and provide evidence in support of the hydrated mineral interpretation of the observations.

The X complex is consistently identified in the two taxonomies recently developed based on CCD spectra acquired in the visible (Bus & Binzel 2002) or in the visible and near infrared range (DeMeo et al., 2009), even though there is not a direct one-to-one correspondence between the Bus and Tholen classes. For instance 92 Undina (Tholen M-type), and 65 Cybele (Tholen P-type) are both classified as Xc-type in the Bus taxonomy. A description of the X complex classes (X, Xk, Xe, Xc) in the Bus & Binzel (2002) classification is summarized in Clark et al. (2004b), while in section 6 we describe the X complex classes in the Bus-DeMeo taxonomy.

Aiming to constrain and understand the composition of the asteroids belong-

ing to the mysterious X group, we have carried out a spectroscopic survey of these bodies in the visible and near infrared range at the 3.5m Telescopio Nazionale Galileo (TNG), in La Palma, Spain, at the 3.5m New Technology Telescope (NTT) of the European Southern Observatory, in La Silla, Chile, and at the Mauna Kea Observatory 3.0 m NASA Infrared Telescope Facility (IRTF) in Hawaii, USA. Results on asteroids classified as E and M-type following the Tholen taxonomy are presented elsewhere (Fornasier et al. 2008, 2010). In this paper we present new VIS-NIR spectra of 24 asteroids belonging to the X type as defined by Tholen & Barucci (1989), that is an "E-M-P" type asteroid for which albedo information was not available at the time of their classification. To constrain their compositions, we conduct a search for meteorite analogues using the RELAB database, and we model the asteroid surface composition with geographical mixtures of selected minerals when a meteorite match is not satisfactory. In addition, we present an analysis of X complex spectral slope values and class distributions in the asteroid main belt, where we include previously published observations of M and E-type asteroids obtained during the same survey (Fornasier et al. 2008, 2010).

2. Observations and Data Reduction

[HERE TABLE 1]

The data presented in this work were mainly obtained during 2 runs (February and November 2004) at the Italian Telescopio Nazionale Galileo TNG of the European Northern Observatory (ENO) in La Palma, Spain, and 2 runs (August 2005, and January 2007) at the New Technology Telescope (NTT) of the European Southern Observatory (ESO), in Chile. Two asteroids (92 Undina, 275 Sapiientia), investigated in the visible range at the NTT and TNG telescopes, were separately

observed in the near infrared at the Mauna Kea Observatory 3.0 m NASA Infrared Telescope Facility (IRTF) in Hawaii during 2 runs in July 2004 and September 2005 (Table 1). We had a total of 11 observing nights. Here we present the results of our observations of 24 X-type asteroids: for 16 objects we obtained new visible and near-infrared wavelength spectra (VIS-NIR), for one object we obtained only a near-infrared spectrum (NIR), and for 7 objects we obtained only visible range spectra (VIS).

The instrument setups are the same as used in Fornasier et al. (2008, 2010). We refer the reader to those papers for complete descriptions of observations and data reduction techniques. The spectra of the observed asteroids, all normalized at $0.55 \mu\text{m}$, are shown in Figs. 1–4, and the observational conditions are reported in Table 1.

[Here Figs 1,2,3, and 4]

To analyze the data, spectral slope values were calculated with linear fits to different wavelength regions: S_{cont} is the spectral slope in the whole range observed for each asteroid, S_{UV} in the $0.49\text{--}0.55 \mu\text{m}$ range, S_{VIS} is the slope in the $0.55\text{--}0.80 \mu\text{m}$ range, S_{NIR1} is the slope in the $1.1\text{--}1.6 \mu\text{m}$ range, and S_{NIR2} is the slope in the $1.7\text{--}2.4 \mu\text{m}$ range. Values are reported in Table 2. Band centers and depths were calculated for each asteroid showing an absorption feature, following the Gaffey et al. (1993) method. First, a linear continuum was fitted at the edges of the band, that is at the points on the spectrum outside the absorption band being characterized. Then the asteroid spectrum was divided by the linear continuum and the region of the band was fitted with a polynomial of order 2 or more. The band center was then calculated as the position where the minimum of the spectral reflectance curve occurs, and the band depth as the minimum in the ratio of the

spectral reflectance curve to the fitted continuum (see Table 3).

[HERE TABLE 2]

[HERE TABLE 3]

3. Spectral Analysis and Absorption Features

The observed asteroids show very different spectral behaviors (Figs 1– 4). Eleven asteroids show at least one absorption feature (Table 3).

50 Virginia (see Fig. 1 and Table 3) shows spectral features centered at 0.43, 0.69, and 0.87 μm (Table 3) associated with aqueous alteration products (Vilas et al. 1994, Fornasier et al. 1999), and seems to be a typical 'hydrated' C-type asteroid.

Five asteroids (50 Virginia, 283 Emma, 337 Devosa, 517 Edith, and 1355 Magoeba) show a weak band at 0.43 μm . For 50 Virginia, 283 Emma, and 517 Edith, the band might be associated with an Fe^{3+} spin-forbidden transition in the iron sulfate jarosite, as suggested by Vilas et al. (1993) for low-albedo asteroids. For 337 Devosa and 1355 Magoeba, the band might be associated with chlorites and Mg-rich serpentines, as suggested by King & Clark (1989) for enstatite chondrites, or to clinopyroxenes such as pigeonite or augite as suggested by Busarev (1998) for M-asteroids.

The 1355 Magoeba spectrum also shows a band centered at $\sim 0.49 \mu\text{m}$ that resembles the absorption seen on some E-type (subclass EII) asteroids (Fornasier & Lazzarin 2001; Fornasier et al. 2007b; 2008, Clark et al. 2004a), where it is attributed to sulfides such as oldhamite and/or troilite (Burbine et al. 1998, 2002a, 2002b). Nevertheless, the estimated albedo of 1355 Magoeba has a moderate value (0.267 ± 0.095 , Gil-Hutton et al. 2007) more consistent with a Tholen M-

type classification.

92 Undina has a very weak band centered at $\sim 0.51 \mu\text{m}$ that is similar to the Fe^{2+} spin-forbidden crystal field transitions in terrestrial and lunar pyroxenes (Burns et al. 1973, Adams 1975, Hazen et al. 1978). This band has been previously detected by Busarev (1998) in the spectra of two M asteroids, 75 Eurydike and 201 Penelope.

An absorption feature has been identified in the $0.9 \mu\text{m}$ region in the spectra of 4 X-type asteroids that have albedos placing them in the Tholen M-class (92 Undina, 337 Devosa, 417 Suevia, and 1124 Stroobantia). The band center ranges from $0.86 \mu\text{m}$ to $0.92 \mu\text{m}$ with a band depth (as compared to the continuum) of 3–6 %. Also 522 Helga, having a low albedo (4%) consistent with the Tholen P-type classification, exhibits a faint band centered at $0.94 \mu\text{m}$. This band was previously reported by several authors in the spectra of Tholen M, E and X-type asteroids (Hardersen et al. 2005; Clark et al. 2004a, 2004b, Fornasier et al. 2008, 2010) and is attributed to low-Fe, low-Ca orthopyroxene minerals.

A peculiar feature centered at $1.6 \mu\text{m}$ was found on the spectrum of 758 Man-cunia. This band resembles one seen on 755 Quintilia (Fornasier et al., 2010, Feiber-Beyer et al. 2006) whose interpretation is still unknown. No bands due to silicates in the 0.9 and $1.9 \mu\text{m}$ regions have been identified in our spectra, except for a change in slope at around $0.77 \mu\text{m}$.

Finally, 1122 Nieth shows a strong $0.96 \mu\text{m}$ absorption band (depth of 24%) and a steep slope in the NIR region, typical of olivine-rich bodies.

Several asteroids of this survey were observed previously by other authors. Five X-type asteroids (50 Virginia, 283 Emma, 337 Devosa, 517 Edith, and 909

Ulla) of the Clark et al. (2004b) survey of the X complex were also studied in this work. The spectral behavior for these objects looks quite similar, except for 283 Emma (our spectrum is flat in the NIR, while the Clark et al. spectrum has a concave shape with a higher spectral gradient), and 909 Ulla (our spectrum has a higher spectral gradient as compared to the Birlan et al. (2007) and the Clark et al. (2004b) spectra). Ockert-Bell et al. (2008, 2010) presented near-infrared spectra of 77 Frigga and 758 Mancunia, that look slightly different compared to ours. In particular, they detect faint spectral bands in the 0.9 and 1.9 μm region for 758 Mancunia, and in the 0.9 μm region for 77 Frigga, bands that are not detected in our spectra. 1355 Magoeba and 3447 Burckhalter were observed in the visible range by Carvano et al. (2001), and their data look very similar to ours.

In sum, comparing our spectra with those in the existing literature, we suggest that asteroids 77 Frigga, 283 Emma, 909 Ulla, and 758 Mancunia may display surface variability as they show different spectral behaviors throughout independent observations. For 758 Mancunia this variability is confirmed also by radar measurements that show the radar cross-section and the polarization ratio to vary considerably with rotation phase (Shepard et al. 2008). For the other 3 asteroids, we cannot exclude that some spectral differences may be linked with unresolved observational differences (such as background stars, or undetected troubles in removing the atmosphere).

4. Tholen Taxonomic Classification

Our targets were classified as belonging to the Tholen X class on the basis of their spectra from 0.4 to 1 μm and because their albedos were not known at the time of classification. Since the original X-type classification in the Tholen

taxonomy, the albedo value has become available for most of the asteroids we observed (Tedesco et al., 2002). Taking into account this important information, together with the visible and near infrared (when available) spectral behavior, we suggest a re-classification of the X-type asteroids in our sample following the Tholen-classification scheme. The suggested new classifications are reported in Table 2.

1122 Nieth (Fig. 4), initially classified as X-type in the Tholen taxonomy, has atypical spectral properties that diverge from all other asteroids. The near infrared spectrum of Nieth clearly shows a strong $0.96 \mu\text{m}$ absorption band and a steep slope in the NIR region. We infer that this asteroid belongs to the olivine-rich A-types (used in the Tholen, Bus, and Bus-DeMeo taxonomic systems).

1328 Devota has a very steep featureless red spectrum. Considering its low albedo value (4%), Devota falls within the D class in the Tholen taxonomy (Fig. 4).

We suggest that the ten asteroids (77 Frigga, 92 Undina, 184 Dejopeja, 337 Devosa, 417 Suevia, 741 Botolphia, 758 Mancunia, 1124 Stroobantia, 1146 Biarmia, and 1355 Magoeba) with moderate albedo values (0.1–0.3) are M-type asteroids while those with albedos lower than 10% fall in the C/P classes. To discriminate between C and P-type asteroids, we analyzed spectral slope values in the visible range (S_{VIS} from 0.55 to $0.80 \mu\text{m}$) and searched for the UV drop-off below $\sim 0.5 \mu\text{m}$ that is typical of C-type asteroids. Comparing the S_{VIS} slopes with the S_{UV} slopes (calculated from 0.49 to $0.55 \mu\text{m}$) of the low albedo asteroids, we find two distinct distributions correlated with the C and P-classes. The 6 asteroids (50, 220, 223, 283, 536, and 517) having the UV absorption and $S_{vis} < 2\%/10^3\text{\AA}$ belong to the C-type, while the 4 asteroids (275, 463, 522, and 909) having $3 < S_{vis} < 6\%/10^3\text{\AA}$ belong to the P-type. 1902 Shaposhnikov, observed only

in the near infrared range, is probably also a P-type, while 3447 Burckhalter, for which the albedo value is 0.336 ± 0.164 (Gil-Hutton et al. 2007) could possibly be an E-type.

5. Meteorite Spectral Matches and Mixing Models

5.1. Meteorite Analogues

To constrain the possible mineralogies of our asteroids, we conducted a search for meteorite and/or mineral spectral matches. We sought matches only for objects observed across the entire VIS-NIR wavelength range. A complete description of the search methodology can be found in Clark et al. (2010) and Fornasier et al. (2010). We used the publicly available RELAB spectrum library (Pieters 1983), which consisted of nearly 15,000 spectra in November of 2008. RELAB spectra were normalized to 1.0 at $0.55 \mu\text{m}$, and then a Chi-squared value was calculated for each RELAB spectrum relative to the normalized input asteroid spectrum. The RELAB spectra were sorted according to Chi-squared values, and then visually examined for dynamic weighting of spectral features by the spectroscopist. Given similar Chi-squared values, a match that mimicked spectral features was preferred over a match that did not. We visually examined the top 200 Chi-squared matches for each asteroid and we constrain the search for analogues to those laboratory spectra with brightness (reflectance at $0.55 \mu\text{m}$) roughly comparable to the albedo of the asteroid. It must be noted that the asteroid data are disk integrated, which could mask spectral variations due to differences in particle size, mineralogy, or abundance. However the meteorite and mineral spectra are well characterized powders measured under well defined laboratory conditions. It should also be noted that an asteroid's albedo is defined at phase angle zero, whereas meteorites'

reflectance is taken at phase angle $> 5^\circ$. For the asteroid albedo value, we used the IRAS albedo published by Tedesco et al. (2002). For the darker asteroids (below 10% albedo), this is a fairly well-constrained value. The uncertainty for brighter asteroid albedos (above 10% albedo) is relatively larger. To account for this, we filtered out lab spectra if brightness differed by more than $\pm 3\%$ in absolute albedo for the darker asteroids (albedos less than 10%), and we filtered out lab spectra if brightness differed by more than $\pm 5\%$ in absolute albedo for the brighter asteroids (albedos greater than 10%). For example, if the asteroid's albedo was 10%, we searched over all lab spectra with $0.55 \mu\text{m}$ reflectance between 5% and 15%. Once the brightness filter was applied, all materials were normalized before comparison by least-squares.

Our search techniques effectively emphasized the spectral characteristics of brightness and shape, and de-emphasized minor absorption bands and other parametric characteristics. As such, we suggest that our methods are complementary to band parameter studies.

[HERE TABLE 4]

[HERE FIGURES 5 and 6]

The best matches between the observed X-type asteroids and meteorites from the RELAB database are reported in Table 4. We matched only the 15 asteroids observed both in the visible and near infrared range that have published albedo values. Some meteorite matches are quite good, while for some asteroids the best meteorite match we found does not satisfactorily reproduce both the visual and near infrared spectral behavior. In particular our attempt to find a meteorite or mineral match failed for the 3 asteroids 1122 Nieth (A-type), 1328 Devota (D-type), and 1355 Magoeba (M-type).

The best matches we found for 7 moderate albedo M-type asteroids are presented in Figure 5. Two asteroids, 741 Botolphia and 1146 Biarmia were not compared with RELAB spectra due to the lack of near-infrared spectral data. We find that iron or pallasite meteorites are the best matches both for the featureless M-type asteroids and for those having minor absorption bands. This result supports the link between M-type asteroids and iron or pallasite meteorites suggested in the literature by several authors. In this small sample, no enstatite chondrites, which have also been suggested to be linked with M-type asteroids, have been found as the best meteorite analogue.

The strongest analogy we found is between 758 Mancunia and a sample of the iron meteorite Landes which has a large number of silicate inclusions in a nickel-iron matrix. It must be noted that no specific grain-size sampling filter was applied, and of concern is the fact that Mancunia's best match is with a spectrum obtained of the cut slab surface of the Landes iron meteorite.

758 Mancunia has a radar albedo of 0.55 ± 0.14 (Shepard et al. 2008) one of the highest values measured for the asteroids, suggesting a very high metal content. Shepard et al. (2008) also found variations in the radar cross-section and polarization ratio with Mancunia's rotational phase, variations that are not related to shape but to the regolith depth, porosity, or near-surface roughness. The Ockert-Bell et al. (2010) Mancunia spectrum shows absorption bands in the 0.9 and 1.9 μm region, and is found to be similar to the ordinary chondrite Paragould. Our spectrum does not show these features, but a change of slope at 0.77 μm and a faint (1.3% depth) feature centered at 1.6 μm , similar to that observed on 755 Quintilia (Fornasier et al. 2010, Fieber-Beyer et al. 2006), whose origin is not yet understood. Considering both radar and spectral observations, 758 Mancunia

could present an heterogeneous surface composition, with a high metal content but also the presence of some silicates that are not uniformly distributed on the surface.

The Landes iron meteorite sample was found to be the best spectral match also for 337 Devosa, even if the meteorite does not fully reproduced the $0.88\ \mu\text{m}$ absorption band of the asteroid. A similar problem occurred for 417 Suevia and 1124 Stroobantia, where different grain sized samples of the iron meteorite DRP78007 are found to be the best spectral matches, but they did not reproduce the asteroids absorption bands in the $0.9\ \mu\text{m}$ region. We note that grain size effects can play an important role in the spectral behavior of iron-nickel meteorites. In fact Britt and Pieters (1988) found that the spectra of M-type asteroids show good agreement with those of iron meteorites with surface features in the range of $10\ \mu\text{m}$ to $1\ \text{mm}$, that is larger than the wavelength of incident light. Meteorites with these roughness values are diffuse reflectors and show the classic red slope continuum of iron, with practically no geometric dependence on reflection. On the other hand, a decreasing of the meteorite surface roughness changes the reflectance characteristics: complex scattering behavior is seen for roughness in the $0.7\text{-}10\ \mu\text{m}$ range, while for roughness values $< 0.7\ \mu\text{m}$ the reflectance is characterized by two distinct components, the specular one which is bright and red sloped, and the nonspecular one which is dark and flat.

For 77 Frigga we were not able to find any meteoritic/mineral analog within the medium albedo range that could reproduce Frigga's red visible slope and flat near-infrared slope. The best spectral match is shown in Fig. 5. The iron meteorite Chulafinnee models the spectral behavior below $0.55\ \mu\text{m}$ very well, and the albedo

values are similar, however the change in spectral slope around $0.9 \mu\text{m}$ is not reproduced.

For 92 Undina we propose two different meteorites: the best spectral match is with a metal-rich powder sample of the pallasite meteorite Esquel, whose albedo of 0.14 is lower than the 0.25 value of the asteroid. The iron meteorite Babb's Mill was a better numerical fit (minimum chi squared fit) and had a more comparable albedo, but was not favored because Babb's Mill has a near infrared spectrum that is much flatter than that of Undina.

In Figure 6 we present the best matches proposed for six low albedo asteroids. It has long been noticed that reflectance spectra of carbonaceous chondrites are similar to those of the low-albedo asteroids (Gaffey & McCord 1978; Hiroi et al. 1996). In particular, CM meteorites show features due to aqueous alteration processes and are linked to low albedo aqueous altered asteroids like the C and G-types (see Vilas et al. 1994, Burbine 1998, Fornasier et al. 1999). Indeed, all the observed low albedo asteroids are best fit with CM meteorites, either unaltered (50 Virginia and 283 Emma) or altered by heating episodes (275 Sapiientia and 517 Edith) or laser irradiation (522 Helga and 909 Ulla) (see Fig. 6). The CM2 MET00639 meteorite matches very well the visible range spectrum of 50 Virginia and in particular the $0.7 \mu\text{m}$ band attributed to $Fe^{2+} \rightarrow Fe^{3+}$ charge transfer absorptions in phyllosilicate minerals. Nevertheless, the meteorite does not well reproduce the asteroid's near-infrared spectrum. The same meteorite was found as a best match for the near infrared region of 283 Emma, but it does not well reproduce the spectrum in the visible range, where the asteroid is featureless. The absence of the $0.7 \mu\text{m}$ band in the asteroid spectrum led us to discard this as a spectral match.

The P-type asteroids 275 Sappientia and the C-type 517 Edith have as best match two different samples of the Murchison carbonaceous chondrite heated at 600°C (grain size < 63 μm) and 700°C (63 μm < grain size < 125 μm), respectively. It must be noted that at these temperatures the phyllosilicates are dehydrated and transformed into olivine and pyroxene and that the 3 μm hydration band vanishes (Hiroi et al., 1996). Our spectral match may indicate that Sappientia and Edith have no hydrated silicates on their surfaces. If hydrated silicates were originally present, the asteroids may have experienced important thermal episodes that dehydrated them.

The P-type asteroids 522 Helga and 909 Ulla are reproduced by a sample of the CM meteorite Migei after laser irradiation. This meteorite is composed of a black matrix with olivine-rich chondrules, olivine aggregates and individual grains, carbonates, and sulfides (Moroz et al. 2004). Its unaltered spectrum is dark and shows absorption features related to hydrated silicates such as the 2.7-3 μm band, the UV-falloff and a 0.75 μm band. Once irradiated, the meteorite is dehydrated, the absorption bands are significantly weakened (Moroz et al. 2004), and the material remains dark – most probably due to abundant submicron inclusions of Fe-rich phases finely dispersed in the glassy mesostasis (Shingareva et al. 2004). Because laser irradiation is a laboratory technique for simulating micrometeorite bombardment, the spectral match between Helga and Ulla and a laser irradiated sample of CM Migei may indicate that the surfaces of these outer belt asteroids, if composed of CM carbonaceous-like materials, may be spectrally reddish due to micrometeoritic bombardment.

5.2. *Mixing Models*

[HERE FIGURE 7]

[HERE TABLE 5]

To constrain the surface compositions of the investigated X-type asteroids and the materials needed to reproduce the weak $0.9\ \mu\text{m}$ band seen on some spectra we considered geographical (spatially segregated) mixtures of several terrestrial and meteoritic materials in different grain sizes: in particular we took into account all the samples included in the US Geological Digital Spectral Library (<http://speclab.cr.usgs.gov/spectral-lib.html>), in the RELAB database, and in the ASTER spectral library (<http://speclib.jpl.nasa.gov>), together with organics solids (e.g. kerogens by Clark et al. 1993 and Khare et al. 1991; Titan tholins from Khare et al. 1984; and Triton tholins from McDonald et al. 1994) and amorphous carbon (by Zubko et al. 1996). The synthetic spectra were compared with the asteroid spectra, using the known IRAS albedo, and the VIS-NIR spectral behavior and continuum slopes. We present these matches as non-unique examples of how geographical mixtures can be used to explain some of the variety found in X-type asteroid spectra. We do not intend to indicate that these are unique derivations of the composition of these asteroids. Such an inversion requires much more information than we currently possess (grain sizes, optical constants, endmembers present, etc.). Nevertheless, the models we present can provide a first order understanding of possible surface composition.

In Figure 7 and Table 5 we present mixing models for the 4 X-type asteroids showing the $0.9\ \mu\text{m}$ band (this band is attributed to low-Fe, low-Ca orthopyroxene and is not reproduced by the meteorite analogues proposed in Table 4). We also present the low albedo asteroids 517 Edith (for which the spectral match with a heated CM meteorite is poor in the $1\text{--}2\ \mu\text{m}$ region), and 1328 Devota (for which we cannot find any satisfactory meteorite analogue).

As shown in Fig. 5 and discussed in Section 5.2 we did not find a meteorite with a similar albedo value that could match the whole VIS-NIR spectral behavior of 92 Undina. However, we were able to produce a model of the surface of this M-type asteroid with a geographical mixture of 99% of pallasite Esquel and 1% orthopyroxene. This mixture model reproduces the spectral behavior of Undina, however its albedo is much lower (0.14) than that of the asteroid (0.25).

For 337 Devosa the spectral behavior has been reproduced by two different mixtures: one composed of 99% pallasite Esquel and 1% orthopyroxene (for an albedo of 0.14) (red line in Fig. 7), and one composed of 98% pallasite Esquel and 2% goethite (for an albedo of 0.14). 337 Devosa has spectral properties in the VIS-NIR spectral range that are very similar to the M-type asteroid 22 Kalliope (see Fornasier et al. 2010). For these asteroids, the $0.9\ \mu\text{m}$ band is consistent with a small amount of anhydrous silicate (such as orthopyroxene), or with a small amount of goethite (an aqueous alteration product).

For 417 SUEVIA the proposed meteoritic analogue (the iron meteorite DRP78007, Fig. 5) does not fit the observed $0.9\ \mu\text{m}$ band. We found that a geographical mixture of 97% IM DRP78007 (RELAB file cdm47) and 3% orthopyroxene models the asteroid spectral behaviour. The albedo of the mixture is 0.16, a bit lower than the value estimated for SUEVIA (0.20). For 1124 STROOBANTIA the proposed meteorite analogue (metallic meteorite DRP78007) also does not fit the faint $0.9\ \mu\text{m}$ band. For this asteroid, we propose two mixing models. One is a geographical mixture of 98% IM MET101A Odessa and 2% orthopyroxene, with an albedo of 0.13 (blue line in Fig. 7). This model reproduces the asteroid spectrum below $1.4\ \mu\text{m}$ but not the longer wavelengths. Alternatively, a mixture of 96% iron meteorite DRP78007 and 4% olivine (albedo 0.16, red line in Fig. 7) fits STROOBANTIA

beyond $0.6\ \mu\text{m}$, but does not match the spectral region below $0.6\ \mu\text{m}$. Although none of the modeled mixtures reproduces all spectral features (albedo, spectral slopes, band depth, and band center) of the asteroid, our best inference from the modeling is to suggest that the surface composition of Stroobantia is probably consistent with metallic meteorites enriched in silicates.

These results show that a few percent (less than 3%) of orthopyroxenes or goethite added to iron or pallasite meteorites can reproduce the weak spectral features around $0.9\ \mu\text{m}$ seen on some asteroids belonging to the X-complex.

517 Edith shows a flat and featureless spectrum. The observed spectral behavior appears similar to the spectrum of pure amorphous carbon (from Zubko et al., 1996), although we cannot exclude the possibility that a small amount of silicates may be present and masked by the dark and opaque materials.

Considering the low albedo value and the featureless and reddish spectral behavior, we classify 1328 Devota as a D-type. Since the Tagish Lake meteorite is usually considered the best meteorite analog for D-type asteroids (Hiroi et al. 2001), we compared the spectrum of Devota with laboratory spectra of several samples of this meteorite. The spectrum of Devota appears to be redder than that of Tagish Lake. This could be due to the different ages of the asteroids and meteorites. The surface of Devota could be older than the meteorite, and the reddening of the asteroid spectrum could be the result of space weathering processes. Alternatively, the spectral behavior of Devota can be reproduced with a geographical mixture of 94% Tagish Lake meteorite (RELAB file c1mt11) and 6% Triton tholins (from McDonald et al. 1994), resulting in an albedo of 0.02. Our observations of Devota do not cover the wavelengths necessary for detection of the tholin spectral feature at about $3\ \mu\text{m}$, so although we cannot constrain the presence of

tholins with the data in hand, we suggest that some tholin or tholin-like component could be the reddening agent producing the observed spectral slope between 0.5 and 2.5 μm .

6. The X complex: overview and discussion

[HERE TABLE 6 and 7]

[HERE FIGURES 8 and 9]

Our survey devoted to the X-complex asteroids as defined by the Tholen (1984) taxonomy is composed of 78 objects, including the E and M-type asteroids already published in Fornasier et al. (2008, 2010). On the basis of their spectral behavior and albedo values, we classified 22 E-types and distributed them into 3 subclasses I, II, and III, (see Fornasier et al. 2008 and references therein). One of the objects (3447) was originally classified as X-type and was tentatively attributed to the E(I) class in this work, due to its moderately high albedo value but with a high uncertainty. Our survey includes 38 M-types, ten of which (77, 92, 184, 337, 417, 741, 758, 1124, 1146) were originally classified as X-types, 7 C-types (498 Tokio was originally classified as an M-type, and all the others as X-type), 1 D (originally classified as X-type), 5 P-type (originally classified as X-type), 3 A-types (2577, 7579 and 1122 which were originally classified as E-types, and an X-type, respectively), and 2 S-types (5806 and 516, which were originally classified as an E and M-type, respectively). In Fig. 8 we show the spectral slope value S_{VIS} calculated in the visible wavelength range versus the semimajor axis for all the E, M and C/P-types observed. As expected, high albedo E-type asteroids populate mainly the Hungaria region and the inner part of the main belt, while low albedo C and P-types are located mainly in the outer part of the main belt or beyond it,

and M-type are located between 2.4 and 3.2 AU. The mean visible spectral slope for the different E, M and P classes are very similar, as expected (Table 6). In the NIR range, M-type asteroids having a band in the $0.9 \mu\text{m}$ region have mean spectral slope S_{NIR1} and S_{NIR2} values similar to P-type asteroids. These values are higher than those of the M-type asteroids without the $0.9 \mu\text{m}$ band. For the E-type asteroids, observations in the infrared range are available only for a very few objects. We give the NIR mean slope values only for the subtype III (4 asteroids observed in the NIR range: 44 Nysa, 214 Aschera, 317 Roxane, and 437 Rhodia), and the subtype II (64 Angelina, 2867 Steins, and 4660 Nereus), that show the lower S_{NIR1} mean value within the X complex (no data are available in the NIR range for the subtype I).

One M-type asteroid, 77 Frigga, show a very peculiar spectrum, with a near infrared spectrum similar to that of other M-type bodies, but with a very high S_{VIS} value comparable with that of the D-type Devosa. Nevertheless its moderate albedo value allows us to exclude any possible link with dark P or D-types. Also A or S type asteroids have S_{VIS} value similar to that of Frigga, but the absence of any absorption band due to olivine and pyroxene lets us exclude any link with these asteroid classes. As discussed in section 3, Frigga may show surface variability, and the $3 \mu\text{m}$ band, usually associated with hydrated silicates, has been detected on its surface (Rivkin et al., 2000). Polarimetric data reveals that Frigga has a large inversion angle (Gil-Hutton, 2007), implying that the surface is composed of small particles (comparable to the wavelength), and/or of a mixture of particles with high contrast in albedo, like refractory inclusions seen on some carbonaceous chondrites (see Belskaya et al. 2010, and references therein). Our attempt to find a meteorite analogue was unsuccessful as the best match found (the iron meteorite

Chulafinnee) does not satisfactorily reproduce the asteroid spectrum. No radar observations are available for this body. Additional observations of 77 Frigga will be very important to confirm its surface heterogeneities and possibly to constrain its surface composition.

In our sample 43 objects were observed in the complete V+NIR spectral range. Among them 37 have spectral features and albedo values compatible with the X-complex (5 E-types, 29 M-types, and 3 P-types). For all objects we investigated the spectral matches with meteorites/minerals or geographical mixture models. For the 5 E-type asteroids (44, 64, 214, 317 and 437) we found good spectral matches with the enstatite achondrite meteorites, in several cases enriched with troilite, oldhamite or orthopyroxenes (Fornasier et al. 2008). The 3 P-type asteroids presented in this paper (275, 522, and 909) exhibit spectral behaviors and albedo values compatible with carbonaceous chondrite meteorites. Most of the M-type asteroids have spectral features and albedo values well represented by iron meteorites, pallasites, and enstatite chondrites – in several cases enriched with orthopyroxenes, olivines, or goethite.

Our new spectral observations enhance the available physical information for the observed asteroids and allow us to apply the Bus-DeMeo classification recently published (DeMeo et al., 2009). The Bus-DeMeo system is based on the asteroids' spectral characteristics over the wavelength range 0.45 to 2.45 μm without taking the albedo into consideration. In the Bus-DeMeo taxonomy, the X complex comprises 4 types (X, Xk, Xe, Xc) as in the Bus & Binzel (2002) system: an asteroid belongs to the Xe-type if the 0.49 μm feature is present, to the Xk-type if a feature is present in the 0.8–1.0 μm range, to the Xc-type if the spectrum is red and featureless with slight concave-down curvature, and to the X-type

if the spectrum is straight and featureless. The Tholen X-type asteroids we observed show different spectral behaviors in the near infrared range. We therefore re-classified 16 of the asteroids presented in this paper and observed both in the VIS and NIR range according to the Bus-DeMeo taxonomy. The corresponding classes are summarized in Table 2. All 5 asteroids showing the faint $0.9\ \mu\text{m}$ band fall in the Xk-type (337 Devosa also has the $0.43\ \mu\text{m}$ band), while 1122 Nieth, which shows a broad and deep $0.96\ \mu\text{m}$ band and a steep infrared spectrum, is classified as an A-type. The 5 asteroids having the $0.43\ \mu\text{m}$ absorption band (note that this region is outside the wavelength limits where the Bus-DeMeo taxonomy is defined) belong to 5 different classes: 337 Devosa is classified as Xk; 50 Virginia, showing bands due to hydrated materials, is a Ch; 283 Emma is a C-type; 517 Edith is an Xc; and 1355 Magoeba, having also the peculiar band at $0.49\ \mu\text{m}$, is classified as Xe-type in the Bus-DeMeo taxonomy. The featureless objects belong to the X-type (77, 758, and 909), D-type (1328, and 1902), and to the C-type (275).

In Table 7 we report Bus-DeMeo taxonomic classifications together with the Tholen classifications (existing or proposed by us) for all the asteroids observed during our survey devoted to the X-complex asteroids. In Fig 9 we show the albedo value versus the semimajor axis for the observed asteroids classified with the Bus-DeMeo taxonomy. We aim to investigate if possible correlations between the classes of this taxonomy and the albedo may exist, although the albedo is not a parameter taken into account in the Bus-DeMeo classification system. We dispose of the albedo value for 7 out of the 10 Xe asteroids, that show the $0.49\ \mu\text{m}$ band typical of this class and attributed to sulfides. Most of them correspond to the high albedo subgroup II of the Tholen E-class, with only two asteroids (132

Aertha and 1355 Magoeba) being classified as M-type in the Tholen taxonomy. So this peculiar band, attributed to the presence of sulfides like oldhamite, seems not to be exclusively associated with high albedo E-type asteroids.

The Bus-DeMeo Xk-class asteroids show two distinct albedo distributions: a high albedo group (albedo > 0.4), corresponding to the subgroup III of the Tholen E-class, and a medium albedo group ($0.1 < \text{albedo} < 0.3$) which includes all the Tholen M-types showing a faint feature in the $0.9 \mu\text{m}$ region. The Xk-class includes also a low albedo object, 522 Helga, that we classified here as a P-type in the Tholen taxonomy. Iron bearing pyroxenes such as orthopyroxene are suggested to cause the feature around $0.9 \mu\text{m}$, characteristic of the Xk class, and seem to be present on asteroids with very different albedo values.

Most of the Bus-DeMeo X-class asteroids have $0.1 < \text{albedo} < 0.2$, with the exception of 504 Cora (albedo = 0.34, therefore classified as E[I] asteroid) and 909 Ulla (albedo=0.034, therefore classified as Tholen P-type). All the C-types have low albedo values, but the Xc and D-types span low and moderate albedo values. In particular the asteroid 849 Ara has a steep spectral slope and falls in the D class according to the Bus-DeMeo taxonomy (Fornasier et al. 2010), but its albedo is very high (0.27), excluding a surface composition of organic-rich silicates, carbon, and anhydrous silicates as commonly expected on low-albedo Tholen D-type asteroids.

From this comparison, it is evident that the Bus-DeMeo taxonomy is very helpful in constraining the asteroids' surface composition (for example Xk-type means presence of orthopyroxene), in particular when some absorption bands are present on the spectra. But it is clear that the asteroid albedo is also a very important parameter for constraining the surface properties and also their evolution

in time (space weathering effects). We strongly encourage the development of a next-stage Bus-DeMeo taxonomy that includes the important albedo parameter for asteroid composition/classification.

7. Summary

We present new visible and near infrared spectra of 24 asteroids belonging to the X-type as defined by Tholen & Barucci (1989), that is an "E–M–P" type asteroid for which albedo information was not available at the time of their classification. The X complex in the Tholen taxonomy is comprised of the E, M and P classes which have very different mineralogies but which are spectrally similar with featureless spectra in broadband visible wavelengths. Our observations reveal a large variety of spectral behaviors within the X class, and we identify weak absorption bands on 11 asteroids. We combine our spectra with the albedo values available since 2002 for the observed bodies to suggest new Tholen-like classifications. We find: 1 A-type (1122), 1 D-type (1328), 1 E-type (possibly, 3447 Burckhalter), 10 M-types (77, 92, 184, 337, 417, 741, 758, 1124, 1146, and 1355), 5 P-types (275, 463, 522, 909, 1902), and 6 C-types (50, 220, 223, 283, 517, and 536). Four new M-type asteroids (92 Undina, 337 Devosa, 417 Suevia, and 1124 Stroobantia) show a faint band in the $0.9\ \mu\text{m}$ region, attributed to low calcium, low iron orthopyroxene. Indeed, several works based on spectral and radar observations show that not all the M-type asteroids have a pure metallic composition (Fornasier et al. 2010 and reference therein).

Three low albedo asteroids (50 Virginia, 283 Emma, and 517 Edith) show a weak band centered at $0.43\ \mu\text{m}$ that we interpreted as due to Fe^{3+} spin-forbidden transition in hydrated minerals (hematite, goethite). Also the medium albedo bodies

337 Devosa and 1355 Magoeba have the same absorption. In this case the band may be associated with chlorites and Mg-rich serpentines or pyroxene minerals such as pigeonite or augite. 50 Virginia shows also two absorptions centered at ~ 0.69 and $0.87 \mu\text{m}$ which are typical of hydrated silicates.

We performed a search for meteorite and/or mineral spectral matches between the asteroids observed in the visible and near infrared range (with published albedo values) and the RELAB database.

The best matches found for all the M-types of our sample are iron or pallasite meteorites as suggested in the literature, however we note that these meteorites often do not reproduce the faint absorption band features (such as the possible orthopyroxene absorption bands at $0.9 \mu\text{m}$) detected on the asteroids. We tried to constraint the asteroids' surface compositions using geographical mixing models for new M-types having the $0.9 \mu\text{m}$ feature. We found good spectral matches by enriching the iron or pallasite meteorites with small amounts ($< 3\%$) of orthopyroxene or goethite. For the low albedo asteroids we found as the best match CM carbonaceous chondrites, either unaltered or altered (submitted to heating episodes or laser irradiation). Our sample includes also two objects whose spectra diverge completely from other X complex asteroids: 1328 Devota, a low albedo body with a red featureless spectrum, suggested to belong to the D-type, and 1122 Nieth, a medium albedo asteroid with a broad and deep $0.9 \mu\text{m}$ band and a steep infrared spectrum, suggested to belong to the A-type. A synthetic model made with the Tagish Lake meteorite, considered as the best meteorite analogue of D-type asteroids (Hiroi et al 2001), and a reddening agent (Triton tholin) reproduces the spectral behavior of 1328 Devota.

The whole sample of asteroids included in our work is 72 X-type objects (we

exclude the A, D and S/Sq-type asteroids), partly published here and partly already published in Fornasier et al. (2008) and Fornasier et al. (2010). The analysis of this complete sample has clearly shown that, although the mean visible spectral slopes of M-, E- and P-type asteroids are very similar to each other, the differences in albedo indicate major differences in mineralogy and composition.

Acknowledgment

The authors thank Dr. M. Ockert-Bell, Dr. M. Shepard, and Dr. A. Migliorini for their help with observations, and A. W. Rivkin and an anonymous referee for their comments and suggestions. BEC thanks Jonathan Joseph for computer programming assistance. SF thanks Dr. F. DeMeo for her help in the classification of the observed asteroids using her taxonomy. Taxonomic type results presented in this work were determined, in whole or in part, using a Bus-DeMeo Taxonomy Classification Web tool by Stephen M. Slivan, developed at MIT with the support of National Science Foundation Grant 0506716 and NASA Grant NAG5-12355. This research utilizes spectra acquired with the NASA RELAB facility at Brown University.

References

Adams, J. B. 1975. Interpretation of visible and near-infrared reflectance spectra of pyroxenes other rock-forming minerals. In *Infrared and Raman Spectroscopy of Lunar and Terrestrial Minerals* (C. Karr, Jr., Ed.), pp. 90–116. Academic Press, New York.

Belskaya, I. N., Fornasier, S., Krugly, Yu. N., Shevchenko, V. G., Gaftonyuk, N. M., Barucci, M. A., Fulchignoni, M., Gil-Hutton, R., 2010. Puzzling asteroid

21 Lutetia: our knowledge prior to the Rosetta fly-by. *Astron. and Astroph.* 515, A29

Birlan, M., Vernazza, P., Nedelcu, D. A., 2007. Spectral properties of nine M-type asteroids. *Astron. Astroph.* 475, 747–754

Britt, D.T., Pieters, C. M., 1988. Bidirectional reflectance properties of iron-nickel meteorites. In: *Lunar and Planetary Science Conference*, 503–512

Burbine, T.H., 1998. Could G-class asteroids be the parent bodies of the CM chondrites? *Meteoritics & Plan. Sci.* 33, 253–258

Burbine, T. H., Cloutis, E. A., Bus, S. J., Meibom, A., Binzel, R. P., 1998. The detection of troilite (FeS) on the surfaces of E-class asteroids. *Bull. Am. Astron. Soc.* 30, 711

Burbine, T. H., McCoy, T. J., Nittler, L., Benedix, G., Cloutis, E., Dickenson, T. 2002a. Spectra of extremely reduced assemblages: Implications for Mercury. *Meteorit. Planet. Sci.* 37, 1233–1244

Burbine, T.H., McCoy, T.J., Meibom, A., 2002b. Meteorite parent bodies. In *Asteroids III* (Bottke, W. et al. editors), pp 653–664, Univ. of Arizona Press, Tucson

Burns, R. G., D. J. Vaughan, R. M. Abu-Eid, M. Witner, and A. Morawski 1973. Spectral evidence for Cr^{3+} , Ti^{3+} , and Fe^{2+} rather than Cr^{2+} , and Fe^{3+} in lunar ferromagnesian silicates. In *Proc. 4th Lunar Sci. Conf.* 983–994

Bus, S. J., Binzel, R. P., 2002. Phase II of the Small Main-Belt Asteroid Spectroscopic Survey A Feature-Based Taxonomy. *Icarus* 158, 146–177

Busarev, V. V., 1998. Spectral Features of M-Asteroids: 75 Eurydike and 201 Penelope. *Icarus* 131, 32–40

Carvano, J. M., Lazzaro, D., Mothé-Diniz, T., Angeli, C. A., Florczak, M.,

2001. Spectroscopic Survey of the Hungaria and Phocaea Dynamical Groups. *Icarus* 149, 173–189

Clark, R.N., Swayze G.A., Gallagher, A.J., King, T.V.V., Calvin, W.M., 1993. U.S. Geological Survey Open File Report 93-592, <http://speclab.cr.usgs.gov>

Clark, B.E., Bus, S.J., Rivkin, A.S., McConnochie, T., Sander, J., Shah, S., Hiroi, T., Shepard, M., 2004a. E-Type asteroid spectroscopy and compositional modeling, *JGR* 109, 1010–1029

Clark, B.E., Bus, S.J., Rivkin, A.S., Shepard, M., Shah, S., 2004b. Spectroscopy of X-type asteroids. *Astron. J.* 128, 3070–3081

Clark, B.E., J. Ziffer, D. Nesvorny, H. Campins, A. S. Rivkin, T. Hiroi, M.A. Barucci, M. Fulchignoni, R. P. Binzel, S. Fornasier, F. DeMeo, M. E. Ockert-Bell, J. Licandro, T. Moth-Diniz, 2010. Spectroscopy of B-Type Asteroids: Subgroups and Meteorite Analogs. *Journal of Geophysical Research*, 115, E06005

Cloutis, E. A., Gaffey, M. J., Smith, D. G. W., Lambert, R. St. J., 1990. Metal Silicate Mixtures: Spectral Properties and Applications to Asteroid Taxonomy. *J. Geophys. Res.*, 95, 281, 8323–8338

Dahlgren, M., Lagerkvist, C. I., 1995. A study of Hilda asteroids. I. CCD spectroscopy of Hilda asteroids. *Astron. Astrophys.* 302, 907–914

Dahlgren, M., Lagerkvist, C.I., Fitzsimmons, A., Williams, I. P., Gordon, M., 1997. A study of Hilda asteroids. II. Compositional implications from optical spectroscopy. *Astron. Astrophys.* 323, 606–619

DeMeo, F. E., Binzel, R. P., Slivan, S. M., Bus, S. J., 2009. An extension of the Bus asteroid taxonomy into the near-infrared. *Icarus* 202, 160–180

Fieber-Beyer, S. K., Gaffey, M. J., Hardersen, P. S., 2006. Near-Infrared Spectroscopic Analysis of Mainbelt M-Asteroid 755 Quintilla. 37th Annual Lunar and

Planetary Science Conference, March 13-17, 2006, League City, Texas, abstract no.1315

Fornasier, S., Lazzarin, M., Barbieri, C., Barucci, M.A., 1999. Spectroscopic comparison of aqueous altered asteroids with CM2 carbonaceous chondrite meteorites. *Astron. Astrophys.* 135, 65–73

Fornasier, S., & Lazzarin, M., 2001. E-Type asteroids: Spectroscopic investigation on the 0.5 μ m absorption band. *Icarus* 152, 127–133

Fornasier, S., Dotto, E., Marzari, F., Barucci, M.A., Boehnhardt, H., Hainaut, O., de Bergh, C., 2004. Visible spectroscopic and photometric survey of L5 Trojans : investigation of dynamical families. *Icarus* 172, 221–232

Fornasier, S., Dotto, E., Hainaut, O., Marzari, F., Boehnhardt, H., de Luise, F., Barucci, M. A., 2007a. Visible spectroscopic and photometric survey of Jupiter Trojans: Final results on dynamical families. *Icarus* 190, 622–642

Fornasier, S., Marzari, F., Dotto, E., Barucci, M. A., Migliorini, A., 2007b. Are the E-type asteroids (2867) Steins, a target of the Rosetta mission, and NEA (3103) Eger remnants of an old asteroid family? *Astron. Astroph.* 474, 29–32

Fornasier, S., Migliorini, A., Dotto, E., Barucci, M. A., 2008. Visible and near infrared spectroscopic investigation of E-type asteroids, including 2867 Steins, a target of the Rosetta mission. *Icarus* 196, 119–134

Fornasier, S., Clark, B.E., Dotto, E., Migliorini, Ockert-Bell, M., Barucci, M. A., 2010. Spectroscopic survey of M-type asteroids. *Icarus* 210, 655–673

Gaffey, M. J., 1976. Spectral reflectance characteristics of the meteorite classes. *J. Geophys. Res.* 81, 905–920

Gaffey, M. J., McCord, T. B., 1978. Asteroid surface materials - Mineralogical characterizations from reflectance spectra. *Space Sci. Reviews* 21, 555–628

Gaffey, M. J., J. F. Bell, and D. P. Cruikshank 1989. Reflectance spectroscopy and asteroids surface mineralogy. In *Asteroids II* (R.P. Binzel, T. Gehrels, and M. S. Matthews, Eds.), pp. 98–127, Univ. of Arizona Press, Tucson.

Gaffey, M. J., K. L. Reed, and M. S. Kelley 1992. Relationship of E-type Apollo asteroids 3103 (1982 BB) to the enstatite achondrite meteorites and Hungaria asteroids. *Icarus* 100, 95–109

Gaffey, M. J., Burbine, T. H., Piatek, J. L., Reed, K. L., Chaky, D. A., Bell, J. F., Brown, R. H., 1993. Mineralogical variations within the S-type asteroids class. *Icarus* 106, 573–602

Gaffey, M. J., Cloutis, E.A., Kelley, M. S., Reed, K. L., 2002. Mineralogy of Asteroids. In *Asteroids III* (Bottke W. et al. editors), pp. 183-204, Univ. of Arizona Press, Tucson.

Gil-Hutton, R., Lazzaro, D., Benavidez, P., 2007. Polarimetric observations of Hungaria asteroids. *Astron. Astrophys.* 468, 1109–1114

Gil-Hutton, R., 2007. Polarimetry of M-type asteroids. *Astron. Astrophys.* 468, 1127–1132

Gil-Hutton, R., Licandro, J., 2010. Taxonomy of asteroids in the Cybele region from the analysis of the Sloan Digital Sky Survey colors. *Icarus* 206, 729–734

Hardersen, P. S., Gaffey, M. J., Abell, P. A., 2005. Near-IR spectral evidence for the presence of iron-poor orthopyroxenes on the surfaces of six M-type asteroids. *Icarus* 175, 141–158

Hazen, R. M., P. M. Bell, and H. K. Mao 1978. Effects of compositional variation on absorption spectra of lunar pyroxenes. In *Proc. 9th Lunar Planet. Sci. Conf.*, 2919–2934

Hiroi, T., Zolensky, M. E., Pieters, C. M., 1996. Thermal metamorphism of the C, G, B, and F asteroids seen from the 0.7 micron, 3 micron and UV absorption strengths in comparison with carbonaceous chondrites. *Meteoritics and Planet. Sci.* 31, 321–327

Hiroi, T., Zolensky, M. E., Pieters, C.M., 2001. The Tagish Lake Meteorite: A Possible Sample from a D-Type Asteroid. *Science* 293, 2234–2236

Jones, T. D., Lebofsky, L. A., Lewis, J. S., Marley, M. S., 1990. The composition and origin of the C, P, and D asteroids: Water as a tracer of thermal evolution in the outer belt. *Icarus*, 88, 172–192.

Khare, B. N., Sagan, C., Arakawa, E. T., Suits, F., Callcott, T. A., Williams, M. W., 1984. Optical constants of organic tholins produced in a simulated Titanian atmosphere - From soft X-ray to microwave frequencies. *Icarus* 60, 127–137.

Khare, B.N., Thompson, W.R., Sagan, C., Arakawa, E. T., Meisse, C., Gilmour, I. 1991. Optical Constants of Kerogen from 0.15 to 40 micron: Comparison with Meteoritic Organics. In *Origin and Evolution of Interplanetary Dust*, IAU Colloq. 126, eds. A.C. Levasseur-Regours and H. Hasegawa, Kluwer Academic Publishers, ASSL 173, 99.

King, T.V.V., Clark, R.N., 1989. Spectral characteristics of chlorites and Mgserpentines using high resolution reflectance spectroscopy. *J. Geophys. Res.* 94, 13997–14008.

Lupisko, D. F., Belskaya, I. N., 1989. On the surface composition of the M-type asteroids. *Icarus* 78, 395–401.

Magri, C. Nolan, M. C.; Ostro, S. J., Giorgini, J. D., 2007. A radar survey of main-belt asteroids: Arecibo observations of 55 objects during 1999 2003. *Icarus* 186, 126–151.

Margot, J.-L., Brown, M.E., 2003. A low-density M-type asteroid in the main-belt. *Science* 300, 1939–1942.

McDonald, G.D., Thompson, W.R., Heinrich, M., Khare, B.N., Sagan, C. 1994. Chemical investigation of Titan and Triton tholins. *Icarus* 108, 137–145.

Moroz, L. V., Hiroi, T., Shingareva, T. V., Basilevsky, A. T., Fisenko, A. V., Semjonova, L. F., Pieters, C. M., 2004. Reflectance Spectra of CM2 Chondrite Mighei Irradiated with Pulsed Laser and Implications for Low-Albedo Asteroids and Martian Moons. *Lunar Planet. Sci. Conf.* 35, abstract 1279

Mothé-Diniz, T., Carvano, J. M., Lazzaro, D. 2003. Distribution of taxonomic classes in the main belt of asteroids. *Icarus*, 162, 10–21.

Ockert-Bell, M.E., Clark, B.E., Shepard, M.K., Rivkin, A.S., Binzel, R.P., Thomas, C.A., DeMeo, F.E., Bus, S.J., Shah, S., 2008. Observations of X/M asteroids across multiple wavelengths. *Icarus* 195, 206–219.

Ockert-Bell, M.E., Clark, B.E., Shepard, M.K., Isaacs, R.A., Cloutis, E.A., Fornasier, S., Bus, J.S., 2010. The composition of M-type asteroids: synthesis of spectroscopic and radar observations. *Icarus* 210, 674–692.

Ostro, S. J., Campbell, D. B., Chandler, J. F., Hine, A. A., Hudson, R. S., Rosema, K. D., Shapiro, I. I., 1991. Asteroid 1986 DA: Radar evidence for a metallic composition. *Science*, 252, 1399–1404.

Ostro, S. J., Hudson, R. S., Nolan, M. C., Margot, J. L., Scheeres, D. J., Campbell, D. B., Magri, C., Giorgini, J. D., Yeomans, D. K., 2000. Radar observations of asteroid 216 Kleopatra. *Science*, 288, 836–839.

Pieters, C. 1983. Strength of mineral absorption features in the transmitted component of near-infrared reflected light: First results from RELAB, *J. Geophys. Res.*, 88, 9534–9544.

Rivkin, A. S., Howell, E. S., Britt, D. T., Lebofsky, L. A., Nolan, M. C., Branston, D. D., 1995. 3-micron spectrophotometric survey of M- and E-class asteroids. *Icarus*, 117, 90–100.

Rivkin, A.S., Howell, E.S., Lebofsky, L.A., Clark, B.E., Britt, D.T., 2000. The nature of M-class asteroids from 3-m observations. *Icarus* 145, 351– 368.

Rivkin, A. S., Howell, E. S., Vilas, F., Lebofsky L. A., 2002. Hydrated minerals on asteroids: The astronomical record. In *Asteroids III* (Bottke W. et al. editors), pp 235–253, Univ. of Arizona Press, Tucson.

Shepard, M. K., Clark, B. E., Nolan, M. C., Howell, E. S., Magri, C., Giorgini, J. D., Benner, L. A. M., Ostro, S. J., Harris, A. W., Warner, B., et al., 2008. A radar survey of M- and X-class asteroids. *Icarus* 195, 184–205.

Shepard, M. K., Clark, B. E., Ockert-Bell, M., Nolan, M. C., Howell, E. S., Magri, C., Giorgini, J. D., Benner, L. A. M., Ostro, S. J., Harris, A. W., Warner, B., Stephens, R. D., Mueller, M., 2010. A radar survey of M- and X-class asteroids II. Summary and synthesis. *Icarus* 208, 221–237.

Shingareva, T. V., Basilevsky, A. T., Fisenko, A. V., Semjonova, L. F., Korotaeva, N.N., 2004. Mineralogy and Petrology of Laser Irradiated Carbonaceous Chondrite Mighei. *Lunar Planet. Sci. Conf.* 35, abstract 1137

Taylor, S. R., 1992. Solar system evolution: a new perspective. an inquiry into the chemical composition, origin, and evolution of the solar system. In *Solar System evolution: A new Perspective*, Cambridge Univ.Press.

Tedesco, E.F., P.V. Noah, M. Moah, and S.D. Price, 2002. The supplemental IRAS minor planet survey. *The Astronomical Journal* 123, 10565–10585.

Tholen, D.J., 1984. Asteroid taxonomy from cluster analysis of photometry. Ph.D. dissertation, University of Arizona, Tucson.

Tholen, D.J., Barucci, M.A., 1989. Asteroids taxonomy. In: Binzel, R.P., Gehrels, T., Matthews, M.S. (Eds.), *Asteroids II*. Univ. of Arizona Press, Tucson, pp. 298–315.

Vernazza, P., Brunetto, R., Binzel, R. P., Perron, C., Fulvio, D., Strazzulla, G., Fulchignoni, M., 2009. Plausible parent bodies for enstatite chondrites and mesosiderites: Implications for Lutetia's fly-by. *Icarus* 202, 477–486

Vilas, F., Hatch, E.C., Larson, S.M., Sawyer, S.R., Gaffey, M.J., 1993. Ferric iron in primitive asteroids - A 0.43- μm absorption feature. *Icarus* 102, 225–231

Vilas, F., Jarvis, K.S., Gaffey, M.J., 1994. Iron alteration minerals in the visible and near-infrared spectra of low-albedo asteroids. *Icarus* 109, 274–283

Warner, B. D., Harris, A. W., Vokrouhlick, D., Nesvorn, D., Bottke, W. F., 2009. Analysis of the Hungaria asteroid population. *Icarus* 204, 172–182

Zellner, B., M. Leake, J. G. Williams, Morrison, D., 1977. The E asteroids and the origin of the enstatite achondrites. *Geochim. Cosmochim. Acta* 41, 1759–1767.

Zubko, V. G., Mennella, V., Colangeli, L., Bussoletti, E., 1996. Optical constants of cosmic carbon analogue grains - I. Simulation of clustering by a modified continuous distribution of ellipsoids. *MNRAS* 282, 1321–1329.

Tables

Table 1. Observational circumstances for the observed X type asteroids. Solar analog stars named "hip" come from the Hipparcos catalogue, "la" from the Landolt photometric standard stars catalogue, and "HD" from the Henry Draper catalogue

Object	Night	UT _{start}	T _{exp}	Tel.	Instr.	Grism	airm.	Solar Analog (airm.)
Object	Night	UT _{start} (hh:mm)	T _{exp} (s)	Tel.	Instr.	Grism	airm.	Solar Analog (airm.)
50 Virginia	18 Nov. 04	04:45	120	TNG	Dolores	LR-R	1.09	hyades64 (1.4)
50 Virginia	18 Nov. 04	04:49	180	TNG	Dolores	MR-B	1.10	hyades64 (1.4)
50 Virginia	19 Nov. 04	04:23	360	TNG	NICS	Amici	1.07	la98-978 (1.17)
77 Frigga	29 Feb. 04	05:12	90	TNG	Dolores	LR-R	1.33	la107684 (1.20)
77 Frigga	29 Feb. 04	05:15	90	TNG	Dolores	LR-B	1.34	la107684 (1.20)
77 Frigga	1 Mar. 04	05:27	120	TNG	NICS	Amici	1.38	la102-1081 (1.46)
92 Undina	20 Jan 07	04:29	40	NTT	EMMI	GR1	1.69	la98-978 (1.35)
92 Undina	17 Sep. 05	11:37	2560	IRTF	SPEX	Prism	1.15	hyades64 (1.00), la115-270(1.10), la93-101(1.10), la112-1333(1.10)
184 Dejopeja	13 Aug 05	06:13	300	NTT	EMMI	GR1	1.07	HD1835 (1.07)
184 Dejopeja	12 Aug 05	06:59	360	NTT	SOFI	GB	1.11	hip103579 (1.06)
184 Dejopeja	12 Aug 05	07:04	360	NTT	SOFI	GR	1.12	hip103579 (1.06)
220 Stefania	21 Nov. 04	00:13	180	TNG	Dolores	LR-R	1.12	hyades64 (1.05)
220 Stefania	21 Nov. 04	00:17	180	TNG	Dolores	MR-B	1.12	hyades64 (1.05)
223 Rosa	20 Nov. 04	20:58	360	TNG	Dolores	LR-R	1.38	la115-271 (1.16)
223 Rosa	20 Nov. 04	21:05	420	TNG	Dolores	MR-B	1.40	la115-271 (1.16)
275 Sapiientia	13 Aug 05	06:44	480	NTT	EMMI	GR1	1.09	HD1835 (1.07)
275 Sapiientia	12 Jul. 04	08:50	1650	IRTF	SPEX	Prism	1.30	16CyB(1.20), la107-684(1.10) la110-361(1.10)
283 Emma	16 Nov. 04	04:08	180	TNG	Dolores	LR-R	1.08	hyades64 (1.03)
283 Emma	16 Nov. 04	04:13	180	TNG	Dolores	MR-B	1.09	hyades64 (1.03)
283 Emma	19 Nov. 04	01:45	240	TNG	NICS	Amici	1.01	Hyades64 (1.01)
337 Devosa	13 Aug 05	01:31	300	NTT	EMMI	GR1	1.08	HD144585 (1.22)
337 Devosa	12 Aug 05	03:16	280	NTT	SOFI	GB	1.38	hip083805 (1.23)
417 Suevia	13 Aug 05	08:12	600	NTT	EMMI	GR1	1.31	HD1835 (1.07)
417 Suevia	14 Aug 05	06:04	480	NTT	SOFI	GB	1.15	la115-271 (1.15)
417 Suevia	14 Aug 05	06:20	720	NTT	SOFI	GR	1.16	la115-271 (1.15)
463 Lola	20 Nov. 04	23:48	180	TNG	Dolores	LR-R	1.10	hyades64 (1.05)
463 Lola	20 Nov. 04	23:52	240	TNG	Dolores	LR-R	1.11	hyades64 (1.05)
517 Edith	16 Nov. 04	02:42	180	TNG	Dolores	LR-R	1.01	hyades64 (1.03)

Continued on next page

Object	Night	UT _{start}	T _{exp}	Tel.	Instr.	Grism	airm.	Solar Analog (airm.)
517 Edith	16 Nov. 04	02:46	180	TNG	Dolores	MR-B	1.01	hyades64 (1.03)
517 Edith	19 Nov. 04	03:50	360	TNG	NICS	Amici	1.02	Hyades64 (1.01)
522 Helga	14 Aug 05	07:20	600	NTT	SOFI	GB	1.13	la115-271 (1.15)
522 Helga	14 Aug 05	07:38	900	NTT	SOFI	GR	1.12	la115-271 (1.15)
522 Helga	20 Jan 07	02:49	600	NTT	EMMI	GR1	1.67	Hyades64 (1.45)
536 Merapi	20 Nov. 04	22:23	150	TNG	Dolores	LR-R	1.34	la115-271 (1.28)
536 Merapi	20 Nov. 04	22:27	150	TNG	Dolores	MR-B	1.34	la115-271 (1.28)
741 Botolpia	20 Jan 07	04:44	300	NTT	EMMI	GR1	1.70	la98-978 (1.35)
758 Mancunia	13 Aug 05	06:05	180	NTT	EMMI	GR1	1.03	HD1835 (1.07)
758 Mancunia	12 Aug 05	06:40	320	NTT	SOFI	GB	1.05	hip103572 (1.06)
758 Mancunia	12 Aug 05	06:46	320	NTT	SOFI	GR	1.05	hip103572 (1.06)
909 Ulla	20 Nov. 04	04:41	180	TNG	Dolores	LR-R	1.11	hyades64 (1.10)
909 Ulla	20 Nov. 04	04:45	240	TNG	Dolores	MR-B	1.11	hyades64 (1.10)
909 Ulla	21 Nov. 04	05:31	300	TNG	NICS	Amici	1.17	la98-978 (1.17)
1122 Neith	20 Nov. 04	03:28	120	TNG	Dolores	LR-R	1.14	hyades64 (1.10)
1122 Neith	20 Nov. 04	03:31	120	TNG	Dolores	MR-B	1.15	hyades64 (1.10)
1122 Neith	21 Nov. 04	04:19	160	TNG	NICS	Amici	1.32	Hyades64 (1.23)
1124 Stroobantia	20 Nov. 04	03:50	300	TNG	Dolores	LR-R	1.02	hyades64 (1.10)
1124 Stroobantia	20 Nov. 04	03:57	360	TNG	Dolores	MR-B	1.02	hyades64 (1.10)
1124 Stroobantia	21 Nov. 04	04:40	480	TNG	NICS	Amici	1.19	la98-978 (1.19)
1146 Biarmia	20 Nov. 04	20:10	300	TNG	Dolores	LR-R	1.31	la115-271 (1.16)
1146 Biarmia	20 Nov. 04	20:19	300	TNG	Dolores	MR-B	1.34	la115-271 (1.16)
1328 Devota	20 Nov. 04	02:58	300	TNG	Dolores	LR-R	1.01	hyades64 (1.02)
1328 Devota	20 Nov. 04	03:04	300	TNG	Dolores	MR-B	1.02	hyades64 (1.02)
1328 Devota	21 Nov. 04	03:45	480	TNG	NICS	Amici	1.03	la98-978 (1.17)
1355 Magoeba	16 Nov. 04	04:28	300	TNG	Dolores	LR-R	1.30	hyades64 (1.03)
1355 Magoeba	16 Nov. 04	04:34	360	TNG	Dolores	MR-B	1.31	hyades64 (1.03)
1355 Magoeba	19 Nov. 04	03:31	480	TNG	NICS	Amici	1.17	Hyades64 (1.21)
1902 Shaposhnikov	14 Aug 05	08:03	480	NTT	SOFI	GB	1.20	hip113948 (1.17)
1902 Shaposhnikov	14 Aug 05	08:12	480	NTT	SOFI	GR	1.25	hip113948 (1.17)
3447 Burckhalter	20 Nov. 04	02:22	300	TNG	Dolores	LR-R	1.42	hyades64 (1.02)
3447 Burckhalter	20 Nov. 04	02:29	300	TNG	Dolores	MR-B	1.46	hyades64 (1.02)

Table 2: Physical and orbital parameters of the X-type asteroids observed and selected on the basis of the Tholen taxonomy (Tholen, 1984). The Bus and Bus-DeMeo classifications are also reported, together with the new Tholen-like classification proposed here, considering the available albedo values (Tedesco et al. 2002; the albedos marked by ^a come from Gil-Hutton et al. 2007) and the spectral behaviors. The spectral slopes values are also given (S_{UV} calculated in the 0.49–0.55 μm wavelength range, S_{VIS} in the 0.55–0.8 μm range, S_{NIR1} in the 1.1–1.6 μm range, S_{NIR2} in the 1.7–2.4 μm range, S_{cont} in the 0.43–2.40 μm for asteroids with VIS and NIR spectra, and 0.43–0.92 μm for those observed only in the visible range (they are marked with an *).

Asteroid	Bus	Bus-DeMeo	NEW TX	albedo	D (km)	a (AU)	e	i ^o	S_{UV}	S_{Vis}	S_{NIR1}	S_{NIR2}	S_{cont}
50 Virginia	Ch	Ch	C	0.04	99.82	2.6518	0.2838	2.8	1.57±0.74	-0.40±0.54	1.39±0.84	-0.16±0.77	1.05±0.71
77 Frigga	X	X	M	0.14	69.25	2.6674	0.1328	2.4	18.23±1.32	10.16±0.57	2.85±0.87	1.08±0.83	5.37±0.78
92 Undina	Xc	Xk	M	0.25	126.42	3.1895	0.1001	9.9	6.56±0.31	3.15±0.54	2.30±0.76	1.63±0.73	2.46±0.71
184 Dejopeja	X	X	M	0.19	66.47	3.1804	0.0763	1.1	5.05±1.02	3.98±0.55	2.72±0.75	1.38±0.75	2.57±0.71
220 Stephania	C	–	C	0.07	31.12	2.3482	0.2585	7.5	2.14±0.32	0.36±0.55	–	–	0.74±0.72*
223 Rosa	C	–	C	0.03	87.61	3.0920	0.1238	1.9	3.99±0.61	1.76±0.57	–	–	1.86±0.73*
275 Sapientia	C	C	P	0.04	103.00	2.7721	0.1615	4.7	7.49±0.69	4.11±0.57	2.21±0.75	2.13±0.73	2.38±0.72
283 Emma	–	C	C	0.03	148.06	3.0447	0.1499	7.9	2.89±0.77	1.87±0.54	0.38±0.81	0.24±0.79	0.73±0.72
337 Devosa	X	Xk	M	0.16	59.11	2.3835	0.1379	7.8	5.57±1.28	3.95±0.57	3.64±0.77	–	3.58±0.02
417 Suevia	Xk	Xk	M	0.20	40.69	2.8006	0.1331	6.6	5.88±2.33	3.31±0.76	5.94±0.76	2.89±0.81	4.06±0.72
463 Lola	–	–	P	0.08	19.97	2.3988	0.2202	13.4	4.50±0.96	4.11±0.55	–	–	4.08±0.73*
517 Edith	C	Xc	C	0.04	91.12	3.1558	0.1819	3.1	2.61±0.78	1.88±0.54	1.52±0.81	0.89±0.81	1.59±0.71
522 Helga	X	Xk	P	0.04	101.22	3.6287	0.0755	4.4	5.64±1.09	3.79±0.55	3.82±0.78	3.38±0.76	3.59±0.71
536 Merapi	C	–	C	0.04	151.42	3.5016	0.0819	19.4	1.72±0.85	1.16±0.55	–	–	1.13±0.72*
741 Botolphia	X	–	M	0.14	29.64	2.7198	0.0678	8.4	6.37±0.88	3.42±0.54	–	–	3.22±0.74*
758 Mancunia	–	X	M	0.13	85.48	3.1861	0.1518	5.6	6.79±1.05	4.06±0.56	2.53±0.75	1.36±0.73	2.19±0.71
909 Ulla	–	X	P	0.03	116.44	3.5550	0.0959	18.8	5.12±1.54	3.36±0.61	3.20±0.89	1.36±0.85	3.64±0.72
1122 Nieth	–	A	A	0.45	12.01	2.6068	0.2562	4.7	15.42±0.58	8.03±0.58	15.31±1.10	6.18±0.92	8.57±0.76
1124 Stroobantia	–	Xk	M	0.16	24.65	2.9253	0.0344	7.7	2.19±1.23	2.01±0.63	4.73±0.88	3.29±0.87	3.49±0.73
1146 Biarmia	X	–	M	0.22	31.14	3.0511	0.2508	17.0	6.08±0.49	1.92±0.56	–	–	1.78±0.73*
1328 Devota	–	D	D	0.04	57.11	3.5093	0.1407	5.7	10.67±0.96	11.90±0.55	11.70±1.10	7.06±1.01	11.01±0.72
1355 Magoeba	Xe	Xe	M	0.27 ^a	12.90	1.8535	0.0450	22.8	13.42±0.98	5.63±0.55	2.23±0.81	-0.80±0.88	3.61±0.74
1902 Shaposhnikov	–	D	P	0.03	96.86	3.9727	0.2242	12.5	–	–	4.08±0.77	2.29±0.77	–
3447 Burckhalter	Xc	–	E ?	0.34 ^a	15.60	1.9907	0.0285	20.7	16.02±1.32	4.66±0.60	–	–	6.17±0.75*

Table 3: Band center, depth and width for the features detected in the asteroid spectra.

Asteroid	Band Center (μm)	Depth (%)	Width (μm)
50 Virginia	0.6920 ± 0.0070	2.2	0.540–0.839
50 Virginia	0.4310 ± 0.0040	1.1	0.416–0.445
50 Virginia	0.8660 ± 0.0080	1.2	0.823–0.911
92 Undina	0.9050 ± 0.0080	2.9	0.742–1.027
92 Undina	0.5103 ± 0.0050	0.7	0.487–0.531
283 Emma	0.4310 ± 0.0040	1.4	0.417–0.443
337 Devosa	0.8820 ± 0.0080	2.8	0.763–1.017
337 Devosa	0.4280 ± 0.0040	3.0	0.410–0.450
417 Suevia	0.8593 ± 0.0100	5.2	0.730–1.007
517 Edith	0.4300 ± 0.0040	1.5	0.416–0.444
522 Helga	0.9400 ± 0.0070	2.3	0.874–1.004
758 Mancunia	1.5960 ± 0.0060	1.3	1.520–1.705
1122 Nieth	0.9650 ± 0.0080	24.3	0.756–1.564
1124 Stroobantia	0.9170 ± 0.0100	5.9	0.807–1.100
1355 Magoeba	0.4910 ± 0.0070	3.0	0.443–0.543
1355 Magoeba	0.4300 ± 0.0040	1.9	0.417–0.445

Table 4: RELAB Matches (Exp means experimental).

ASTEROID	ALBEDO	BEST FIT	MET CLASS	MET REFL	NAME	GRAIN SIZE
50 Virginia	0.04	PH-D2M-032	CM	0.03	MET00639	<75 μ m
77 Frigga	0.14	MR-MJG-082	IM	0.18	Chulafinnee	
92 Undina	0.25	MR-MJG-083	IM	0.23	Babb's Mill	
92 Undina	0.25	MB-TXH-043-H	Pall	0.14	Esquel	<63 μ m
184 Dejepeja	0.19	MB-TXH-043-H	Pall	0.14	Esquel	<63 μ m
275 Sapiientia	0.04	MB-TXH-064-C	CM Exp.	0.03	Murchison heated to 600°C	<63 μ m
283 Emma	0.03	PH-D2M-032	CM	0.03	MET00639	<75 μ m
337 Devosa	0.16	MB-TXH-046	IM	0.16	Landes	slab
417 Suevia	0.20	MB-TXH-047-D	IM	0.15	DRP78007	75-125 μ m
517 Edith	0.04	MB-TXH-064-D	CM-Exp	0.03	CM Murchison heated to 700°C	63-125 μ m
522 Helga	0.04	MA-ATB-068	CM Exp	0.05	CM Migei Laser Irrad.	<45 μ m
758 Mancunia	0.13	MB-TXH-046	IM	0.16	Landes	slab
909 Ulla	0.03	MA-ATB-068	CM Exp	0.05	CM Migei Laser Irrad.	<45 μ m
1124 Stroobantia	0.16	MB-TXH-047-A	IM	0.12	DRP78007	<25

Table 5: Geographical mixing models. ¹ blue line in Fig. 7, ² red line in Fig. 7

ASTEROID	ALBEDO	GEOGRAPHICAL MODEL	FILE SOURCE	MODEL ALBEDO
92 Undina	0.25	99% pallasite Esquel	RELAB ckmb43	0.14
		1% orthopyroxene	RELAB cbpe40	
337 Devosa ¹	0.16	98% pallasite Esquel	RELAB ckmb43	0.14
		2% goethite	ASTER	
337 Devosa ²	0.16	98% pallasite Esquel	RELAB ckmb43	0.14
		1% orthopyroxene	RELAB cbpe40	
417 Suevia	0.20	97% iron met. DRP78007	RELAB cdmb47	0.16
		3% orthopyroxene	RELAB cbpe40	
517 Edith	0.04	100% amorphous carbon	Zubko et al., 1996	
1124 Stroobantia ¹	0.16	98% iron met. MET101A	RELAB c1sc99	0.13
		2% orthopyroxene	RELAB cbpe40	
1124 Stroobantia ²	0.16	96% iron met. DRP78007	RELAB cdmb47	0.16
		4% olivine	USGS	
1328 Devota	0.04	94% carb. chond. Tagish Lake	RELAB c8mt11	0.03
		6% Trit. Tholin	McDonald et al. 1994	

Table 6: Mean spectral slopes, for the different classes of asteroids with the associated standard deviation value. We discard from the following analysis a few asteroids initially classified as E/M/X in the Tholen taxonomy but whose spectral properties diverge completely from these classes and who have been since reclassified as A, S or D-type (A: 1122, 2577, and 7579; S/Sq: 516, and 5806; D: 1328).

Asteroid Class	Mean S_{VIS} (%/(10^3 \AA))	Mean S_{NIR1} (%/(10^3 \AA))	Mean S_{NIR2} (%/(10^3 \AA))
E (all)	3.92 ± 1.73	—	—
E[I]	4.60 ± 1.18	—	—
E[II]	5.15 ± 1.31	0.85 ± 0.30	0.32 ± 0.15
E[III]	2.43 ± 1.12	1.07 ± 0.81	1.09 ± 0.87
M with the $0.9 \mu\text{m}$ band	3.54 ± 0.90	3.14 ± 1.51	1.82 ± 1.42
M without the $0.9 \mu\text{m}$ band	4.00 ± 1.97	1.73 ± 2.07	0.81 ± 1.21
P	3.34 ± 1.69	2.66 ± 1.65	1.83 ± 1.25
C	1.77 ± 1.94	0.48 ± 0.68	0.17 ± 0.35

Table 7: The Tholen (existing or proposed by this work) and the Bus–DeMeo classification for all the asteroids observed withing our spectroscopical survey of the X complex. 1 = this work, 2 = Fornasier et al. 2010, 3 = Fornasier et al. 2008 and reference therein.

Asteroid	Tholen	Bus-DeMeo	reference	Asteroid	Tholen	Bus-DeMeo	reference
16	M	Xk	2	498	C	Xc	2
22	M	Xk	2	504	E (I)	–	3
44	E (III)	Xk	3	516	S	Sq	2
50	C	Ch	1	517	C	Xc	1
55	M	Xk	2	522	P	Xk	1
64	E (II)	Xe	3	536	C	C	1
69	M	Xk	2	558	M	Xk	2
77	M	X	1	620	E (III)	Xk	3
92	M	Xk	1	741	M	X	1
97	M	Xc	2	755	M	Xk	2
110	M	Xk	2	758	M	X	1
125	M	–	2	785	M	X	2
129	M	Xc	2	849	M	D	2
132	E (II)	Xe	2	860	M	X	2
135	M	Xk	2	872	M	Xk	2
161	M	Xc	2	909	P	X	1
184	M	X	1	1025	E (I)	–	3
201	M	X	2	1103	E (III)	Xk	3
214	E (III)	Xk	3	1122	A	A	1
216	M	Xk	2	1124	M	Xk	1
220	C	C	1	1146	M	X	1
223	C	C	1	1251	E (III)	Xk	3
224	M	Xc	2	1328	D	D	1
250	M	Xk	2	1355	M	Xe	1
275	P	C	1	1902	P	D	1
283	C	C	1	2035	E (II)	Xe	3
317	E (III)	Xk	3	2048	E (II)	Xe	3
325	M	X	2	2449	E (I)	–	3
337	M	Xk	1	2577	A	A	3
338	M	Xk	2	2867	E (II)	Xe	3
347	M	Xk	2	3050	E (III)	Xk	3
369	M	Xk	2	3103	E (II)	Xe	3
382	M	–	2	3447	E (I) ?	Xc	1
417	M	Xk	1	4660	E (II)	Xe	3
418	M	X	2	5806	S	S	3
434	E (II)	Xe	3	466435	E (I)	–	3
437	E (III)	Xk	3	6911	E (II)	Xe	3
441	M	X	2	7579	A	A	3
463	P	–	1	144898	E (I)	–	3

Figure captions

Fig. 1 - Visible and near infrared spectra of X-type asteroids.

Fig. 2 - Visible and near infrared spectra of X-type asteroids.

Fig. 3 - Visible and near infrared spectra of X-type asteroids.

Fig. 4 - Visible and near infrared spectra of X-type asteroids.

Fig. 5 - Best spectral matches between the observed medium albedo asteroids and meteorites from the RELAB database (see Table 4 for details of the meteorite samples). All these asteroids are re-classified as M-type following the Tholen classification scheme. For 92 Undina 2 meteorites are proposed: in red the IM Babb's Mill and in blue the IM Esquel.

Fig. 6 - Best spectral matches between the observed low-albedo asteroids and meteorites from the RELAB database (see Table 4 for details of the meteorite samples).

Fig. 7 - Geographical mixing model for the asteroids 92 Undina, 337 Devosa, 417 Suevia, 517 Edith, 1124 Stroobantia, and 1328 Devota (see details of each model in Table 5).

Fig. 8 - Spectral slope value (S_{VIS}) versus the semimajor axis for the different asteroids observed, classified following the Tholen taxonomy. The size of the symbols is proportional to the asteroids' diameter.

Fig. 9 - Albedo versus semimajor axis for the different asteroids observed, classified following the Bus-DeMeo taxonomy. The size of the symbols is proportional to the asteroids' diameter.

Figures

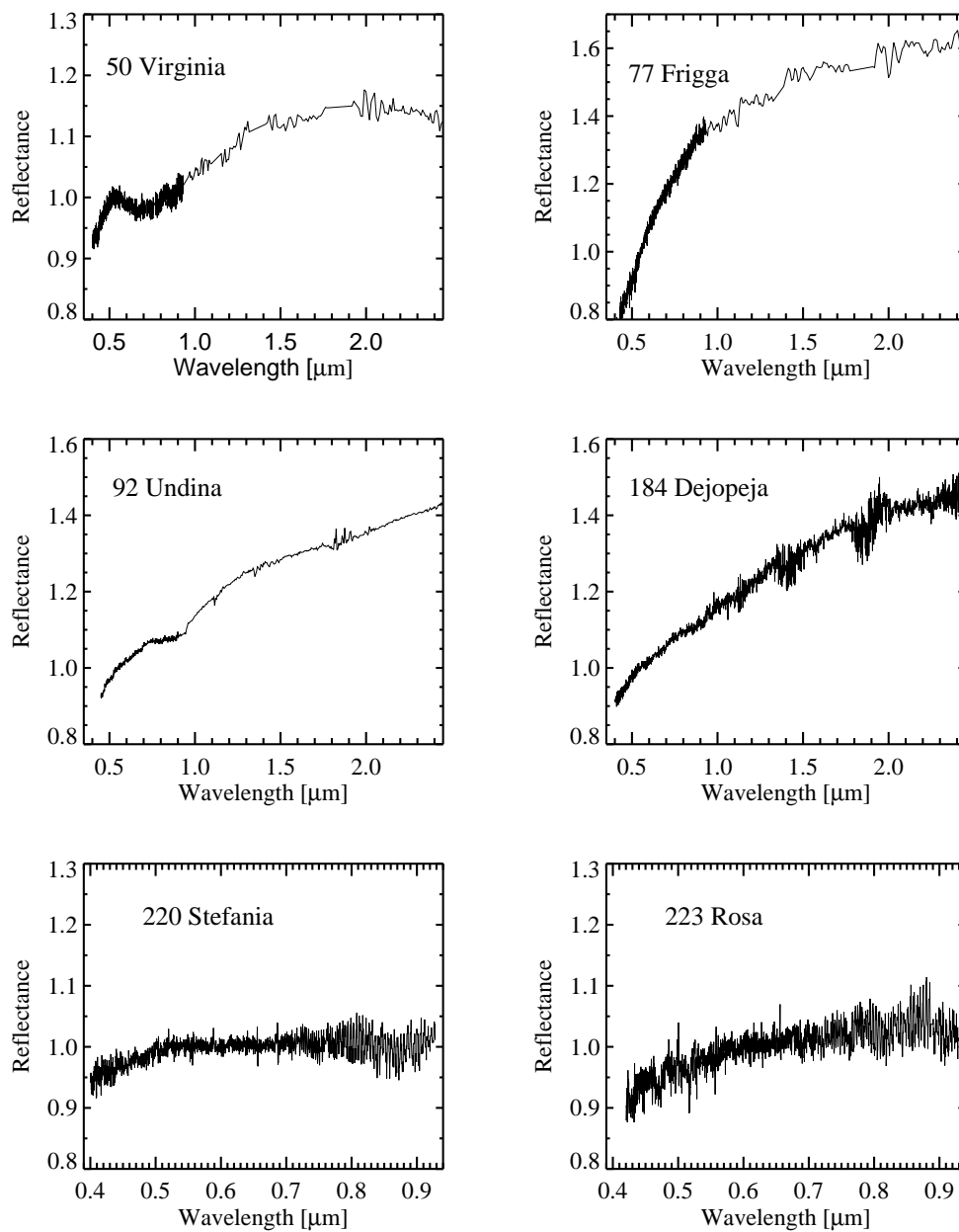


Figure 1:

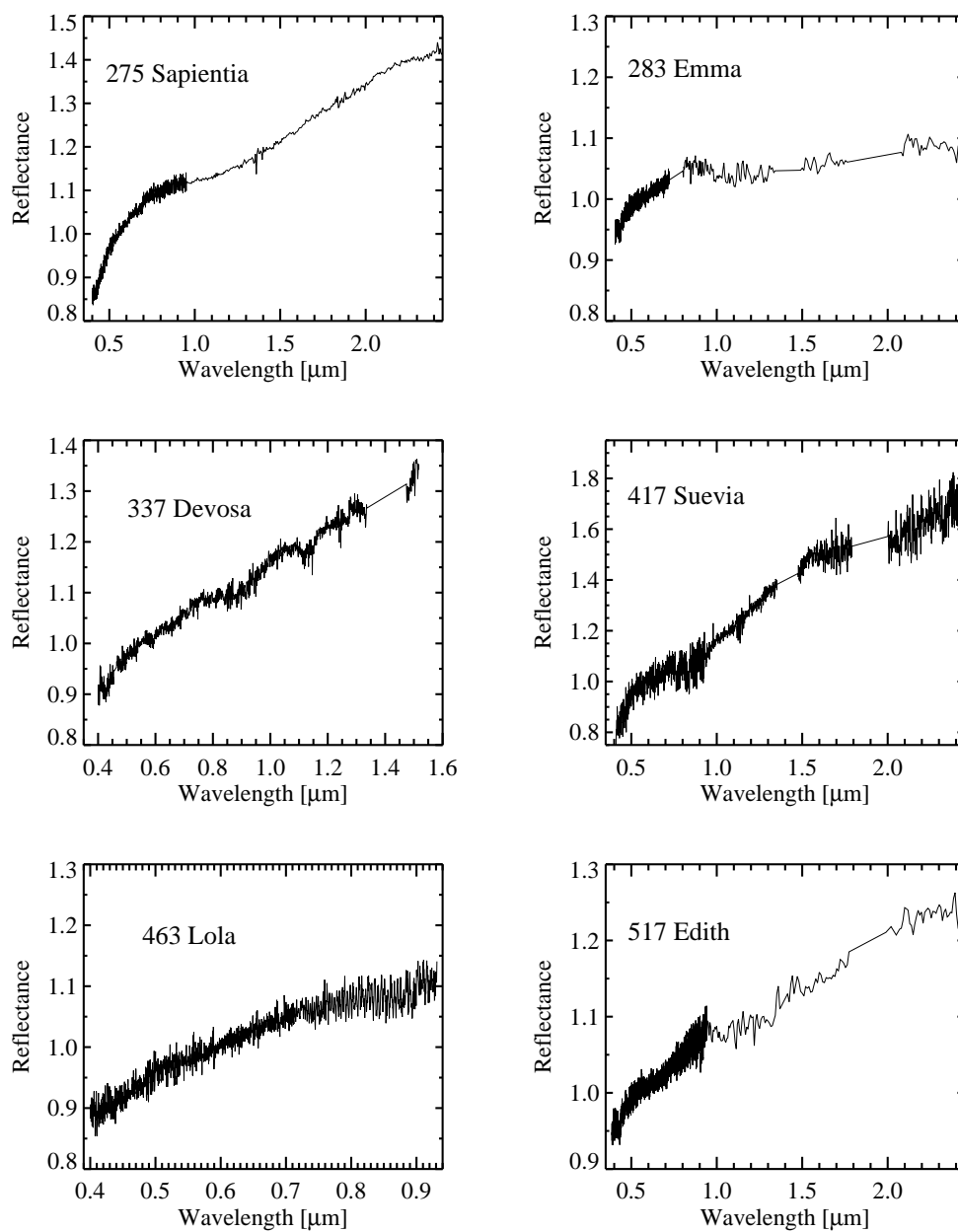


Figure 2:

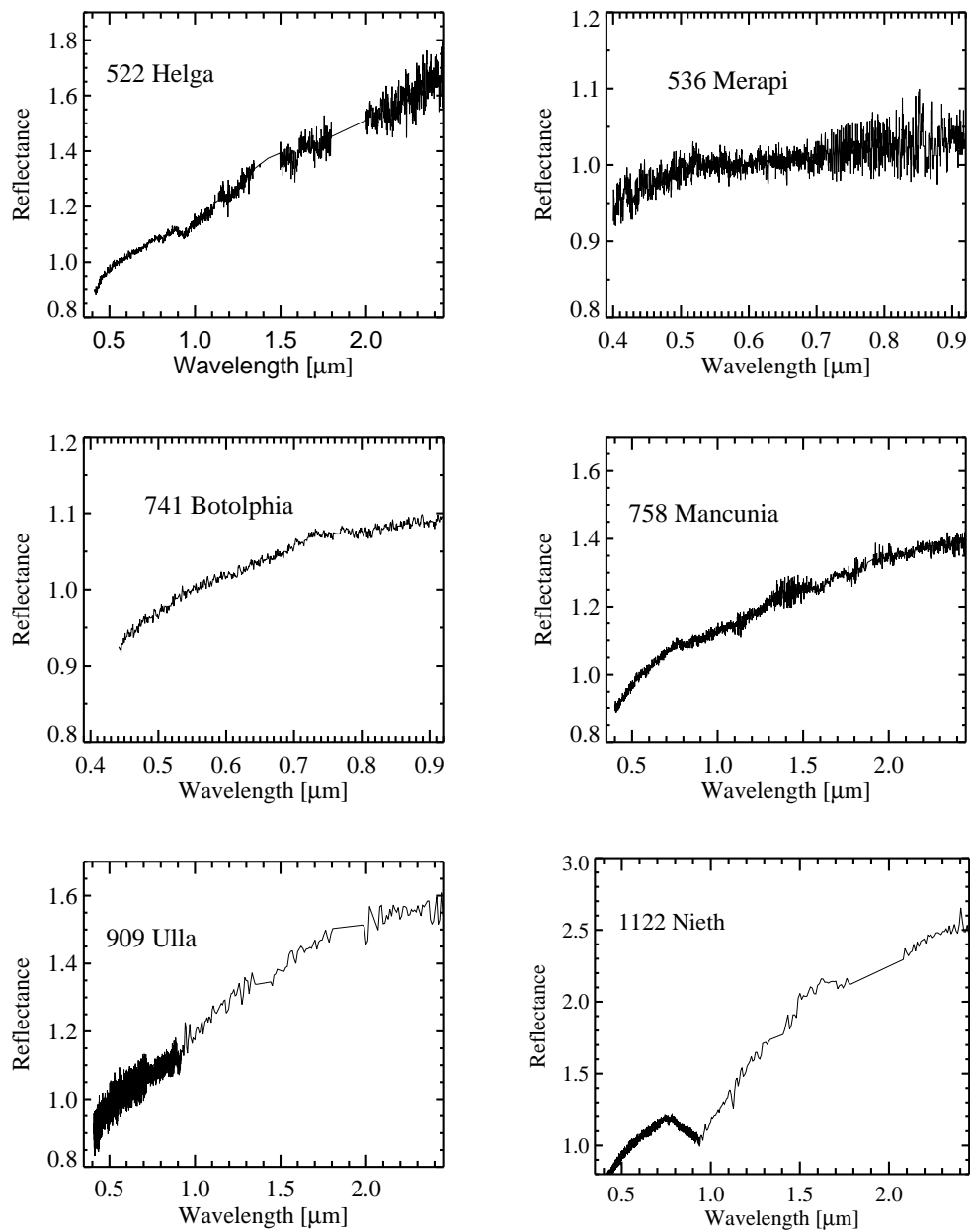


Figure 3:

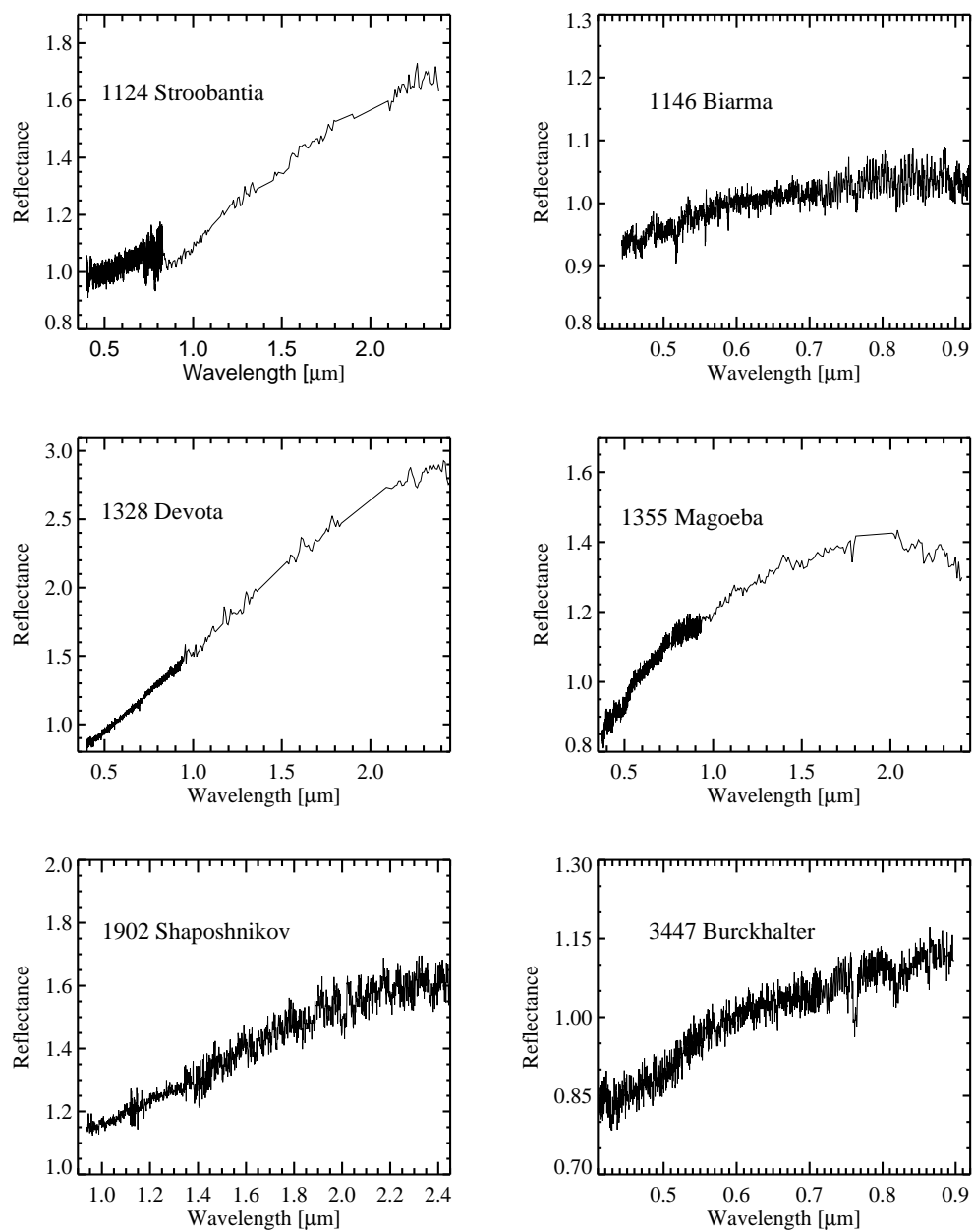


Figure 4:

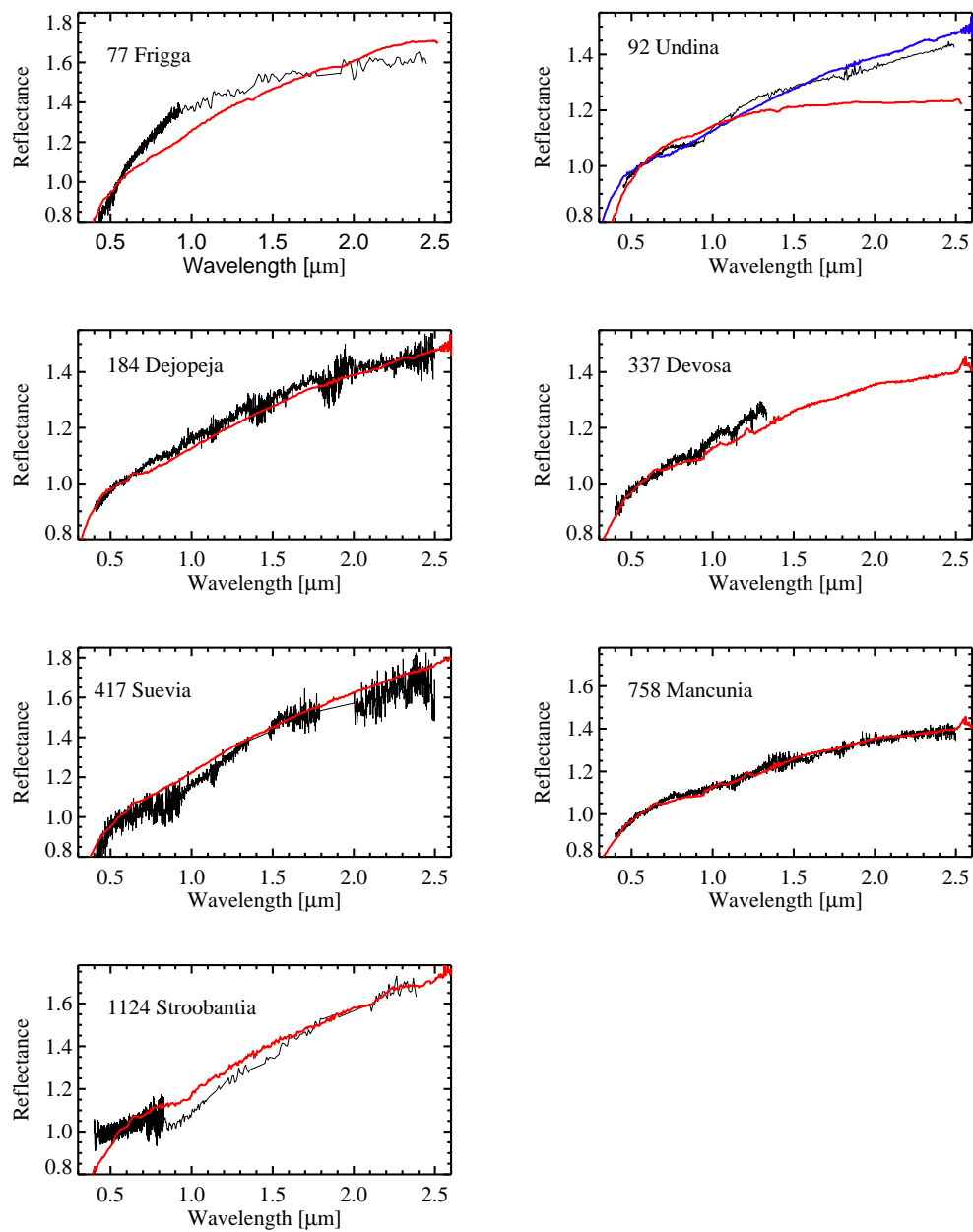


Figure 5:

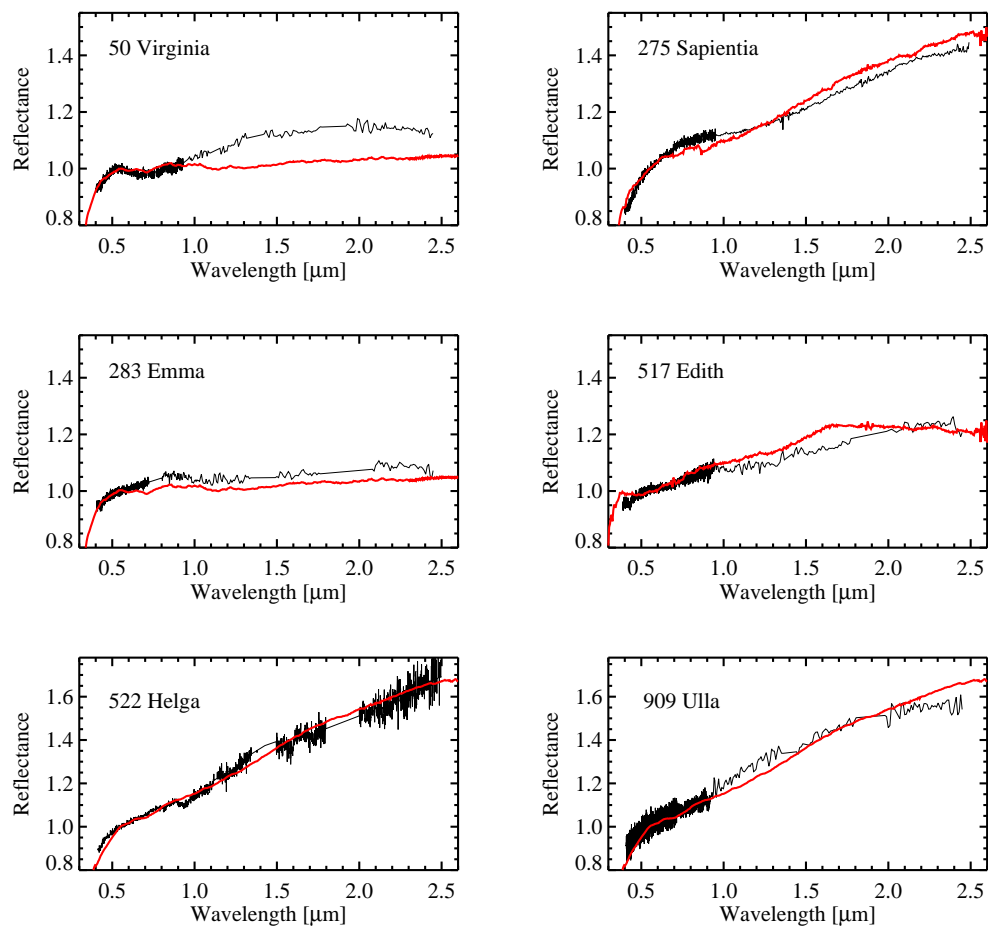


Figure 6:

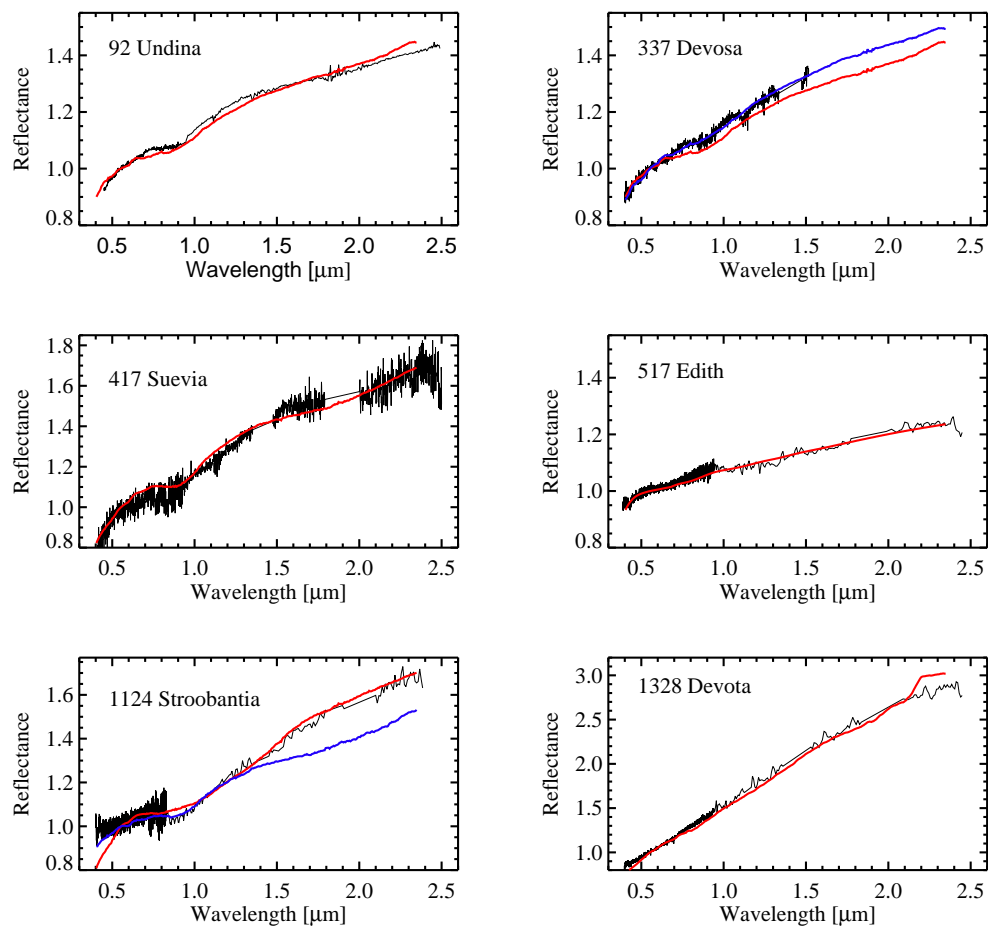


Figure 7:

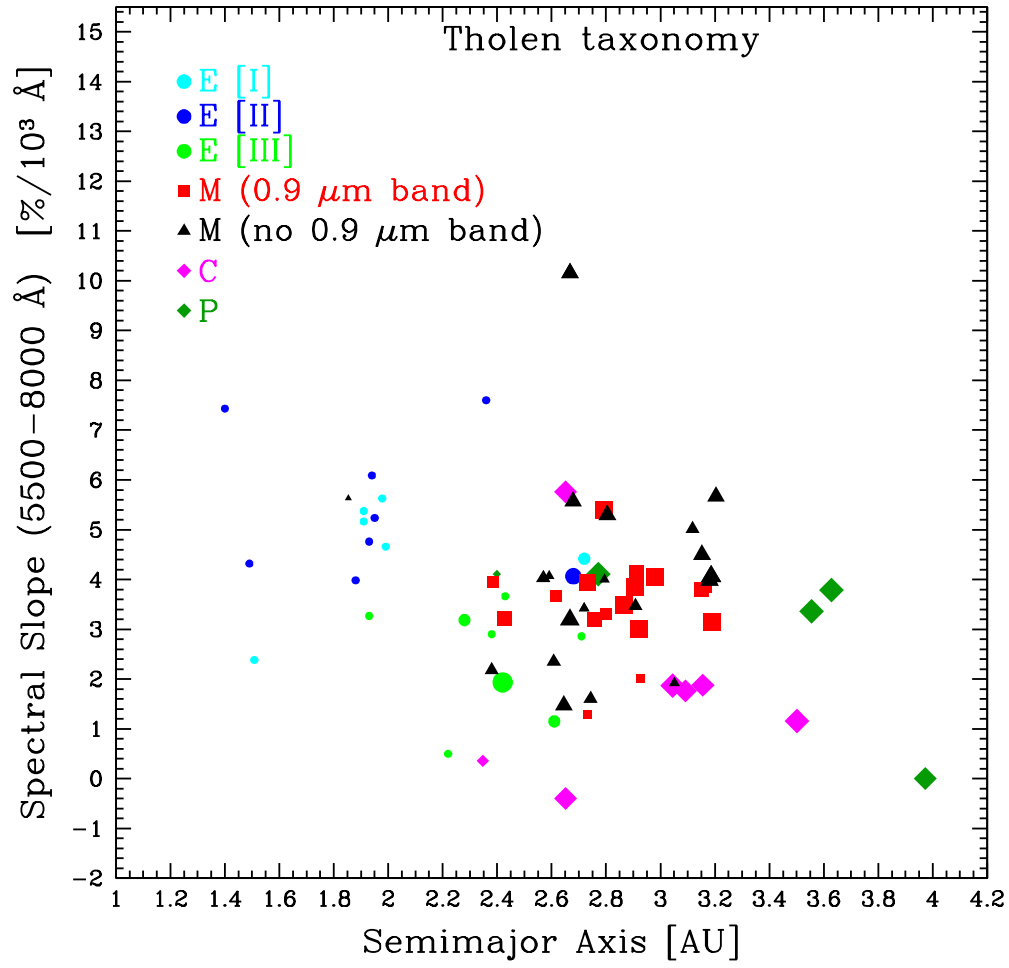


Figure 8:

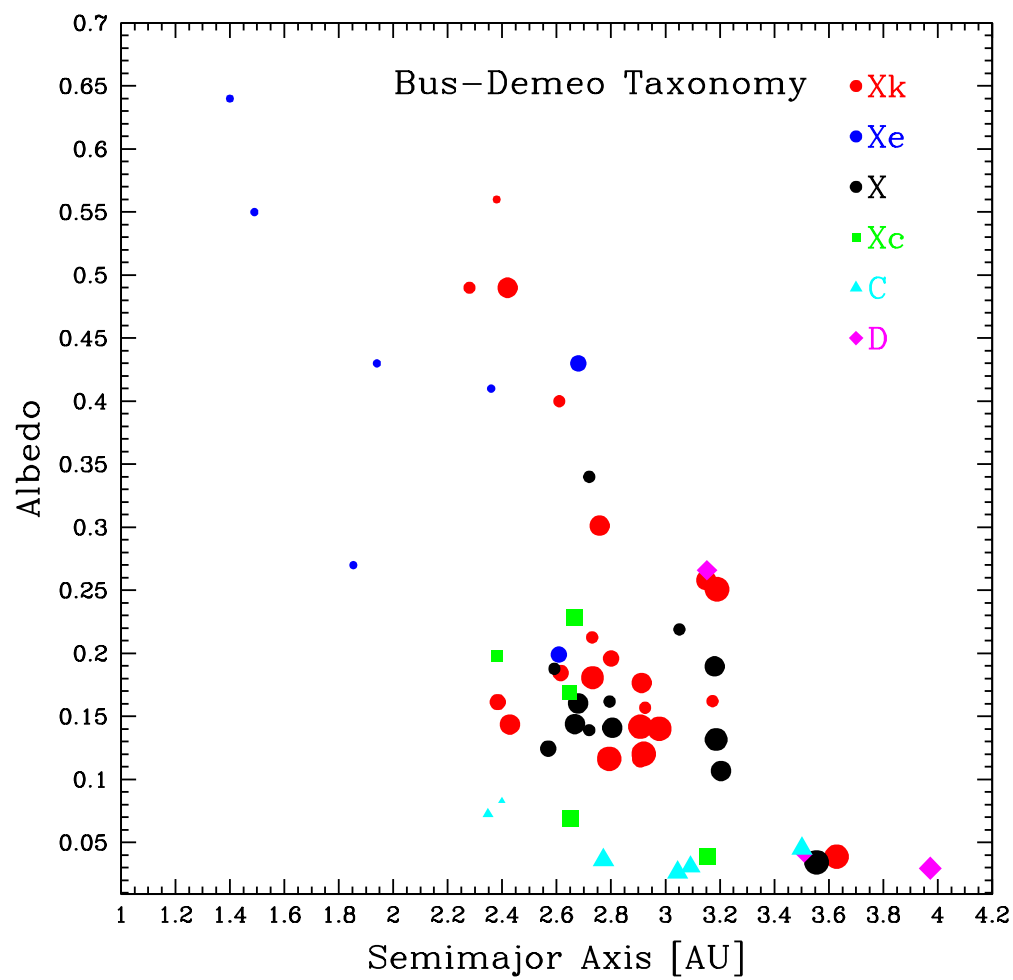


Figure 9: